ERDC/CHL TR-22-7

US Army Corps
of Engineers®
Engineer Research and
Development Center

ERDC
ENGINEER RESEARCH & DEVELOPMENT CENTER

Three-Dimensional Numerical Model Study of Flow near a Scour Hole in Isle of Wight Bay near Ocean City, Maryland

Allen Hammack and Morgan M. Johnston

April 2022

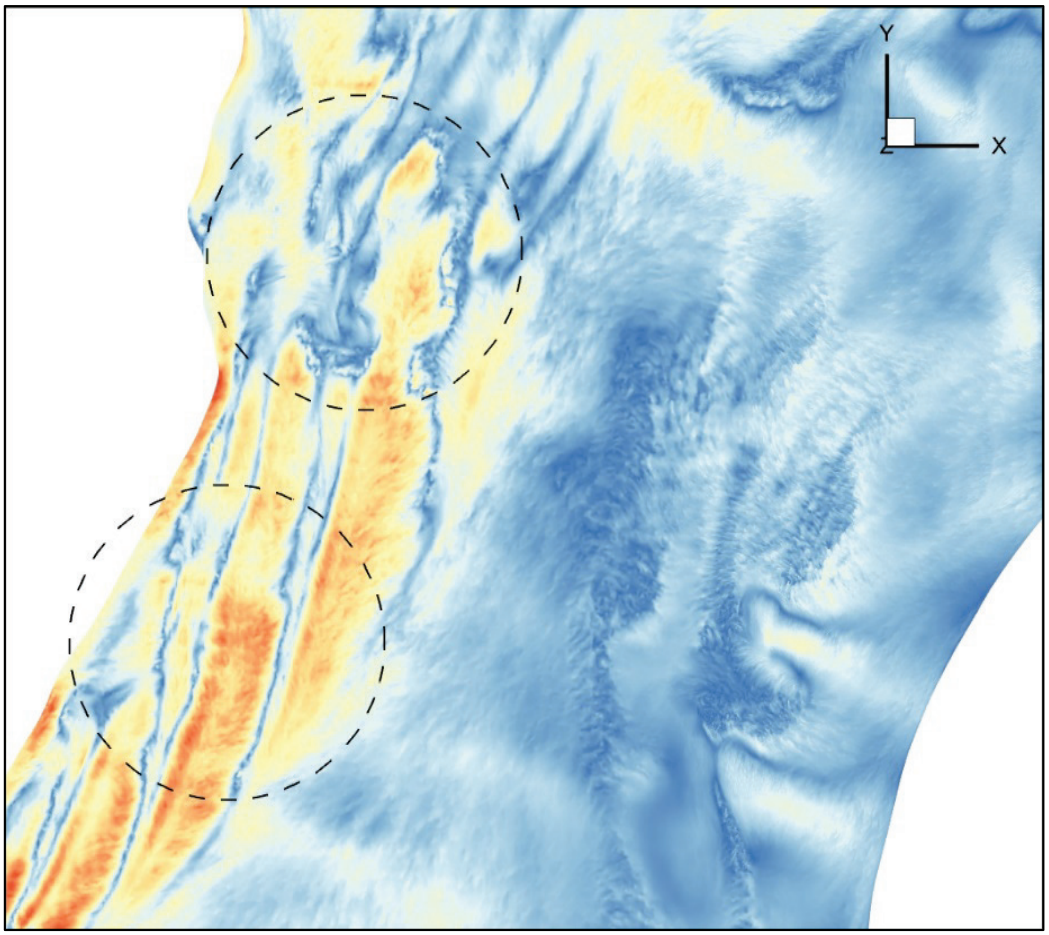

Coastal and Hydraulics Laboratory

The US Army Engineer Research and Development Center (ERDC) solves the nation's toughest engineering and environmental challenges. ERDC develops innovative solutions in civil and military engineering, geospatial sciences, water resources, and environmental sciences for the Army, the Department of Defense, civilian agencies, and our nation's public good. Find out more at www.erdc.usace.army.mil.

To search for other technical reports published by ERDC, visit the ERDC online library at https://erdclibrary.on.worldcat.org/discovery.

ERDC/CHL TR-22-7
April 2022

Three-Dimensional Numerical Model Study of Flow near a Scour Hole in Isle of Wight Bay Near Ocean City, Maryland

Allen Hammack and Morgan M. Johnston

Coastal and Hydraulics Laboratory
US Army Engineer Research and Development Center
3909 Halls Ferry Road
Vicksburg, MS 39180-6199

Final report

Prepared for USACE, Baltimore District
Baltimore, MD 21201

Under USACE, Baltimore District; MIPR E140

Abstract

A scour hole has developed in Isle of Wight Bay near Ocean City, MD. This hole could grow to the point that nearby land developments are threatened, so channel-bed protection measures may be implemented near this scour hole. Appropriately designing those bed protection measures requires knowledge of the flow behavior in the scour hole, so a three-dimensional model study has been conducted to determine the flow behavior at the extreme flood and ebb tides present during a pre-selected month of tide cycles. Steady-state simulations of the flows during those two tide conditions have been completed. Contour plots of the flow velocity near the bed and the corresponding bed shear stresses are provided as input for the design of the bed protection measures.

Contents

Figures and Tables

Figures

Tables

Preface

This study was conducted for the US Army Corps of Engineers, Baltimore District, under MIPR E140.

The work was performed by the Navigation Branch of the Navigation Division, US Army Engineer Research and Development Center, Coastal and Hydraulics Laboratory (ERDC CHL). At the time of publication of this report, Mr. Ben Burnham was chief, Navigation Branch; Ms. Ashley Frey was chief, Navigation Division; and Dr. Julie Rosati, Flood and Coastal Risk Management, was the technical director for Flood and Coastal Systems. The deputy director of ERDC CHL was Mr. Keith Flowers, and the director was Dr. Ty V. Wamsley.

Appreciation is expressed to Mr. Jared McKnight, Dr. Gaurav Savant, and Mr. David S. Smith of the ERDC CHL. Mr. McKnight provided the bathymetry and simulation results from a related study used to develop the flow domain and boundary conditions for this study. Dr. Savant provided guidance on the selection of the boundary locations for the flow domains used. Mr. Smith compiled the version of the flow solver RANS-AdH used for all simulations in this study.

Appreciation is also expressed to Mr. David Dumas of the ERDC Defense Supercomputing Resource Center technical support team. Mr. Dumas provided support with the software used to develop the meshes and ensured that the simulations could be completed in accordance with the project schedule.

In addition, appreciation is expressed to Ms. Anna Hopkins and Ms. Misty Curran of the ERDC CHL Management Integration Office and to Ms. Deby Carraway and Ms. Mary Claire Allison of ERDC CHL. Ms. Hopkins, Ms. Curran, Ms. Carraway, and Ms. Allison provided administrative support for all aspects of this report including the resourcing of funding and the completion of all necessary purchases.

The commander of ERDC was COL Teresa A. Schlosser, and the director was Dr. David W. Pittman.

1 Introduction

1.1 Background

The US Army Corps of Engineers, Baltimore District (NAB), has discovered a scour hole in Isle of Wight Bay near Ocean City, MD. (See the red marker in Figure 1.)

Figure 1. Location of Isle of Wight Bay near Ocean City, MD.

The area of Isle of Wight Bay where the scour hole is located is shown in Figure 2. NAB defined two areas of Isle of Wight Bay near the scour hole that served as the focus of this study. These areas of interest are indicated by the two yellow circles. The diameter of these circles is approximately 250 ft[1]. Figure 3 shows the surrounding bathymetry near the scour hole. This scour hole is very close to developed coastline, and any growth of the scour hole toward the coastline could cause problems for the buildings in the area. NAB is interested in knowing if and in what direction the scour hole is likely to grow. NAB reached out to the US Army Engineer Research and Development Center (ERDC), Coastal and Hydraulics Laboratory, to conduct a numerical model study to determine the flow behavior near the scour hole. This flow field information will be used to inform decisions on how to best prevent scour hole growth toward the coastline.

[1] For a full list of the spelled-out forms of the units of measure used in this document, please refer to *US Government Publishing Office Style Manual*, 31st ed. (Washington, DC: US Government Publishing Office 2016), 248-52, https://www.govinfo.gov/content/pkg/GPO-STYLEMANUAL-2016/pdf/GPO-STYLEMANUAL-2016.pdf.

Figure 2. Areas of interest in Isle of Wight Bay.

Figure 3. Bathymetry in the general vicinity of the scour hole.

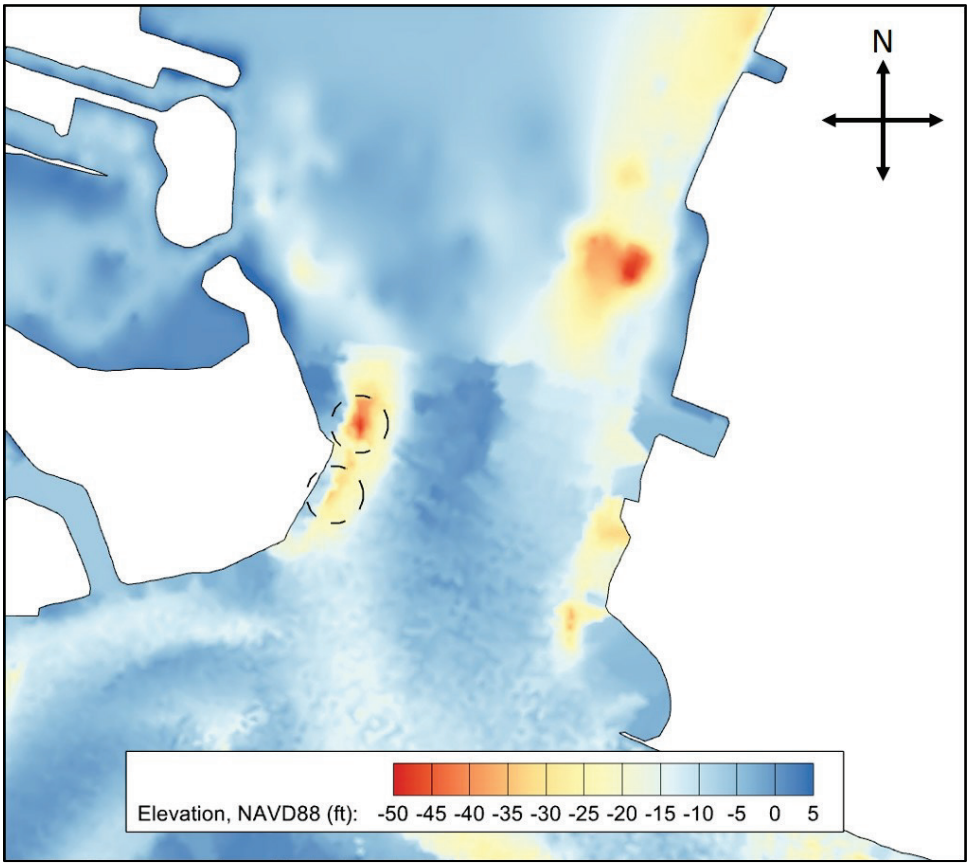

1.2 Objective

The objective of this study is to determine flow field information near the bed — particularly very close to the channel bed — in two areas of interest near the scour hole. The flow field information determined during this study will, in turn, be used by NAB to determine if additional bed protection measures are needed near the scour hole, and if so, the appropriate size and location for that additional bed protection.

1.3 Approach

Near a scour hole such as the one in Isle of Wight Bay, the flow behavior is three-dimensional (3D), so accurately calculating the flow field near a scour hole required a 3D computational flow solver. The ERDC 3D Reynolds-Averaged, Navier-Stokes (RANS) module of the Adaptive Hydraulics (AdH) code was chosen to model the flow behavior in the area around the scour hole. Though the flow in Isle of Wight Bay is tidal, 3D modeling of multiple tide cycles in a 3D RANS code is prohibitively time consuming and computationally expensive. To reduce the computational effort to fit those constraints, steady-state simulations were chosen for this study. Also, steady-state simulations provide the information necessary to determine the appropriate type of bed protection near the scour hole. The flow conditions selected correspond to the most extreme flood and ebb condition during the tide cycle used in a previously completed study that used two-dimensional Shallow-Water (SW2) Adaptive Hydraulics (AdH). For the remainder of the report, the RANS-AdH model is referred to as the *3D model*, and the SW2-AdH model is referred to as the *2D model*. The flow solver itself is referred to as RANS-AdH. The flood and ebb tide simulation have been completed, and the results are included in this report.

2 Modeling Process

Near a scour hole that is very deep compared to the surrounding bathymetry, the flow likely has a significant vertical acceleration. In the scour hole near the western shore of Isle of Wight Bay near Ocean City, MD, the depth of flow increases significantly (approximately 25–30 ft) from the surrounding area, so the vertical flow accelerations are likely non-negligible. (Further details and supporting figures are included in the discussion of the Isle of Wight Bay bathymetry in Chapter 3.) Accurately calculating the flow behavior near such scour holes requires a tool capable of accurately calculating the flow acceleration in all three spatial dimensions. Therefore, a 3D Navier-Stokes (non-hydrostatic) numerical flow model is an appropriate tool for predicting the flows required in this study. (Brunner et al. 2020) The ERDC RANS-AdH code has been used to model the flow behavior in the area around the scour hole. All modules of AdH produce time-varying flow solutions, and steady-state solutions are obtained by simulating the flow field over an amount of time until the dynamic variation in the flow field ceases. (Hammack and Johnston 2019) This chapter is a discussion of the flow equations used by RANS-AdH and the modeling process followed for this study.

2.1 Governing equations

The RANS equations are employed to model the flow field approaching, interacting with, and passing by scour holes. These equations are 3D with four degrees of freedom: the pressure and the three components of fluid velocity. These equations make no assumptions about pressure distributions. Since many hydraulic flow models assume the flow is hydrostatic, RANS models are referred to as *non-hydrostatic models*.

The RANS equations are derived from the conservation of mass and conservation of momentum applied to fluid flow by decomposing the instantaneous flow velocity into a mean component, $\boldsymbol{U}$, and a fluctuating component, $\boldsymbol{u}$, and averaging these equations over time periods that are long compared to the periods of the fluctuations. Mathematically, the conservation of mass for an incompressible fluid is described as

$$\nabla \cdot \boldsymbol{U} = 0 \tag{1}$$

and the conservation of momentum is given as

$$\rho\left(\frac{\partial U}{\partial t} + \boldsymbol{U}\cdot\nabla\boldsymbol{U}\right) - \nabla\cdot\sigma + \nabla\cdot(\rho\boldsymbol{u}\boldsymbol{u}) = 0 \tag{2}$$

where

t = time
ρ = fluid density
$\sigma = -p\boldsymbol{I} + \tau$
p = flow pressure
$\boldsymbol{I}$ = identity matrix
$\tau = 2\mu\boldsymbol{\Gamma}$
$\boldsymbol{\Gamma} = \frac{\mathbf{1}}{\mathbf{2}}(\nabla\boldsymbol{u} + \nabla\boldsymbol{u}^{\boldsymbol{T}})$
μ = fluid viscosity.

The RANS equations are written in terms of the mean velocity, $\boldsymbol{U}(x, t)$, and pressure, $p(x, t)$, to reduce the modeling of turbulence to a set of quasi-steady-state equations that incorporate terms to model the effects of turbulence on the main flow. In a RANS approach, the term $\nabla\cdot(\rho\boldsymbol{u}\boldsymbol{u})$ is used to represent the effect of turbulence on the mean flow.

Using a Boussinesq treatment, an eddy viscosity added to the molecular viscosity in the momentum equations accounts for the turbulent effects. (Wilcox 1998). An eddy viscosity model that uses a single value throughout the flow domain has been used to replicate the turbulent effects. The eddy viscosity can be thought of as the *stiffness* of the flow. Large eddy viscosity values produce flows that do not have enough diffusion, which will significantly distort the flow behavior. Therefore, during the simulation process, the eddy viscosity value was gradually reduced until the velocities no longer changed with decreasing values of the eddy viscosity. This threshold value of eddy viscosity was used for all simulations.

The flow resistance due to the boundaries of the flow domain is included in the flow domain with the surface roughness coefficient. The boundary layer is not modeled directly, but the wall effects are modeled using the law of the wall (Schlichting and Gersten 2000):

$$u = \frac{u_\tau}{\kappa}\ln\frac{y}{y_0} \tag{3}$$

where

u = velocity parallel to the boundary
u_τ = friction velocity (also referred to as the shear velocity)
κ = von Kármán constant
y = distance normal to the boundary
y_o = roughness height.

AdH uses an automatic mesh adaption scheme to ensure that the flow solution is independent of the mesh resolution. This mesh adaption is controlled through two parameters: a mesh refinement tolerance and the maximum number of levels of mesh refinement. The mesh refinement tolerance is a parameter that combines the flow information (pressure, velocity, etc.) into a single parameter, which reduces the amount of information the user must specify when determining when to adapt the mesh.

During a simulation, a residual value is calculated and outputted for each node in the flow domain at each time step. This residual value can be thought of as an estimate of the *error* of the flow calculation. The refinement tolerance, which the user specifies during the simulation set-up process, is the value of this residual above which AdH will refine a mesh element. The mesh adaptation scheme used in RANS-AdH is the same adaptation technique used in the shallow-water modules of AdH (SW2-AdH and SW3-AdH). (More information on the mesh adaptation scheme used in RANS-AdH can be found at https://www.erdc.usace.army.mil/Locations/CHL/AdH/ .)

2.2 Modeling procedure

Before the equations of motion can be applied, the domain must be defined into discrete portions. This discretization process includes the construction of a 3D CAD representation of the flow domain including the bathymetry, an estimate of the water surface, and vertical boundaries encompassing the plan area extents. The CAD model is then used as input for a mesh generator.

A computational mesh is constructed to fill the volume enclosed by the CAD model surfaces. For any AdH simulation, the computational mesh must only sufficiently describe the flow domain boundaries because automatic mesh refinement ensures that the flow features inside the flow

domain are reproduced correctly. The mesh of the CAD surfaces is composed of individual faces of the elements that form the flow domain boundaries. The extents of these boundaries are chosen based on the areas of interest in the study and the boundary condition information available. Flow information such as velocity, discharge, and pressure are needed at these boundaries to determine a particular solution to the governing partial differential (RANS) equations.

The proper modeling procedure uses the automatic mesh adaption to ensure a mesh-independent flow solution has been obtained. The maximum number of levels of refinement specified should be large enough that the mesh residual calculated after adaption is reduced to a value below the refinement tolerance before reaching the maximum number of adaption levels specified by the user. Setting up the automatic mesh adaption for a simulation requires the mesh residual information from a solution on the initial mesh (the mesh created with enough resolution to sufficiently recreate the boundaries of the flow domain and provide a reasonable rough estimate of the flow field). Once a simulation has been completed on the initial mesh, the user must choose a value of the refinement tolerance and the maximum number of levels of refinement to begin the mesh adaption. During the adaption simulation, AdH will identify elements with mesh residual values that exceed the refinement tolerance and refine those elements. The flow solution and a new residual will be calculated using the mesh with the refined elements. Then, the mesh residual will be calculated and compared to the refinement tolerance to determine if a further level of adaption will be applied. This refinement process is repeated until either the residual values throughout the mesh are below the refinement tolerance or the maximum number of levels of refinement has been reached.

For any AdH simulation, a solution is calculated for a particular instant in time, and the solution progresses by stepping through time. How much simulated time for which a simulation should be run depends on the flow behavior and the information that the user is trying to gain from the simulation results. For this study, the steady-state behavior of the flows near the two areas of interest is sought to determine what shear stresses are produced so appropriate bed protection can be chosen. Therefore, all simulations in this study were run until a steady-state solution was obtained.

The steady-state simulation can then be compared to existing field data in the area of interest to determine whether the model reproduces the flow behavior in real life. Field measurements corresponding to the tide cycles from the 2D study (used to determine the flow conditions for this 3D study) were unavailable when this study was completed. For this study, the appropriateness of the modeling procedure and accuracy of the results are ensured by using the geometry from and applying boundary conditions from the 2D study, which has been validated to field data. Furthermore, the modeling procedure taken ensures that the flow solution is both mesh independent and independent of further lowering of the eddy viscosity.

3 Flow Domain Development

Before the simulations can begin, a representation of the relevant geometry must be created. For this study, the relevant geometry is the flow domain, which is defined by a CAD file. This study involves 3D simulations, so the CAD must also be 3D. Once the CAD geometry has been developed, the volume of the flow domain must be discretized into a computational mesh for the simulations. This chapter is a discussion of the flow domain geometry development.

3.1 Flow domain development

The computational domain for each 3D simulation in this study consists of the bathymetry, the water surface, the flux boundaries, and the vertical side boundaries. Note that determining the location of the planwise boundaries of the flow domain is highly coupled with the computational meshing concerns described in Chapter 4. Therefore, the placement of the planwise boundaries of the flow domain is completed iteratively in combination with the meshing. For example, a flow domain of sufficient size with appropriate boundary orientations could be developed, but the subsequent meshes generated could be extremely large. Then, the simulations using that mesh could not be completed in an amount of time suitable for the project schedule. In such a case, the size of the flow domain would have to be reduced, and meshing would have to be attempted on the smaller flow domain.

3.1.1 Bathymetry

The bathymetry used was derived from the bathymetry from a previously completed 2D numerical model study of Isle of Wight Bay[1]. The mesh from the 2D simulation was used for the bathymetry surface for each 3D simulation. Using the mesh from the 2D simulations for the bathymetric surface in the 3D simulations promotes consistency among the model for any comparison of the results that may be made to inform decisions on the bed protection near the scour hole. A contour plot of the elevations (in

[1] C. Jared McKnight, Tate O. McAlpin, Keaton E. Jones, and Cassandra G. Ross. In preparation. *Ocean City Inlet, Maryland: A Two Dimensional Shallow Water Adaptive Hydraulics (AdH-SW2D) Hydrodynamic and Sediment Transport Model*. ERDC/CHL Technical Report. Vicksburg, MS: US Army Engineer Research and Development Center.

NAVD88[1] ft) in the area of Isle of Wight Bay considered during the determination of the flow domain for the 3D simulations is shown in Figure 3. The contours range from -50 ft, NAVD88 (shown in red), to 5 ft, NAVD88 (shown in blue). Two areas of particular interest for bed protection are circled. These areas along the western shoreline are the focus of the 3D model study.

3.1.2 Water surface

The top surface was created using depths from the 2D solution to generate a water surface elevation for the two times of interest selected (Section 3.1.4). If the depth calculated at each node in a 2D flow solution is added to the corresponding elevation, the water surface elevation for the entire domain is produced. Using the same element connectivity in the original 2D mesh, this method provided a surface that can be used to represent the water level for each 3D simulation.

3.1.3 Flow domain extents (planwise)

The 2D domain (outlined in orange in Figure 4) is approximately 440,000 ft long by 171,000 ft wide. Because more detailed flow information around the scour hole is sought in this study, much smaller elements are required for the 3D simulations than were used in the 2D simulation. Furthermore, because the vertical flow velocity behavior must be calculated to provide that required flow information sought in this study, the flow domain will be divided vertically, and these vertical divisions significantly increase the amount of mesh elements required. Therefore, for a certain planwise area of Isle of Wight Bay, the 3D simulation will require significantly more mesh resolution than a corresponding 2D simulation. Figure 5 shows the full 2D flow domain extents and closer views of the area of Isle of Wight Bay that was considered for the selection of the flow domain for the 3D simulations.

[1] North American Vertical Datum of 1988

Figure 4. Ocean City 2D flow domain extents.

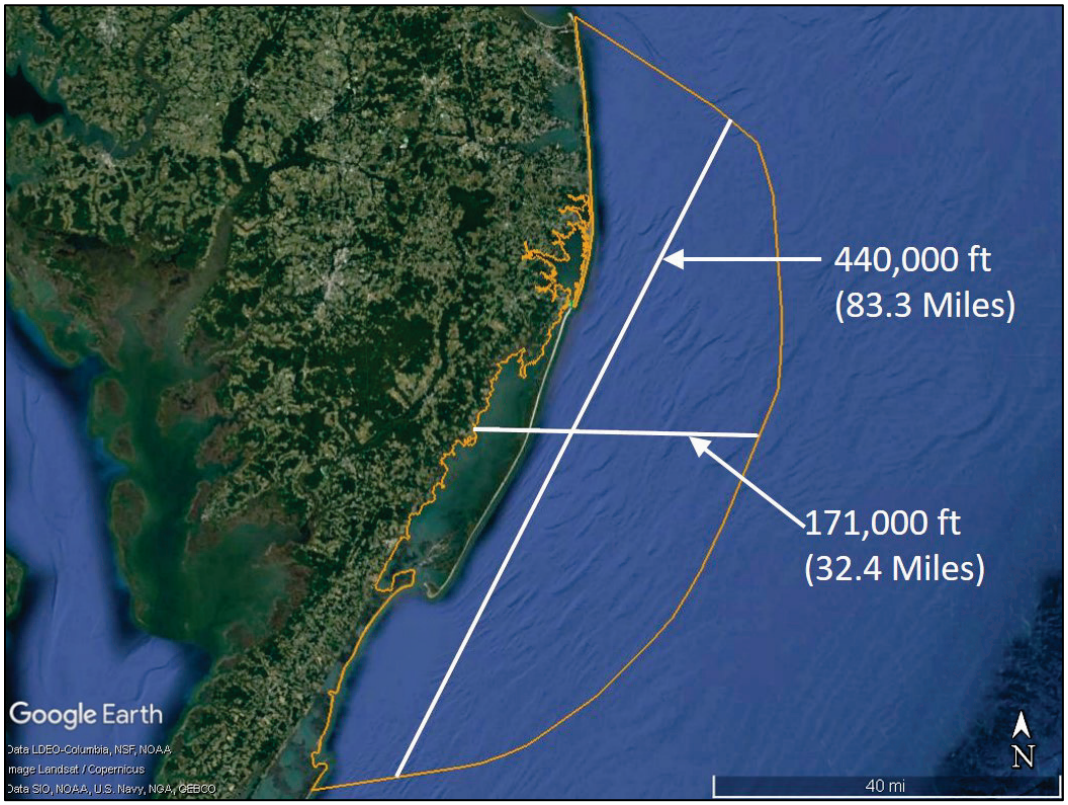

Figure 5. Ocean City 2D model study flow domain extents.

The extents of the flow domain were chosen based on two main criteria:

- the direction of flow from the 2D solution
- the constraints related to the number of nodes and element size in the computational mesh created from the flow domain.

A discussion of how the extents of the 3D flow domains were chosen is included in the following sections.

3.1.4 Flux boundaries

Isle of Wight Bay experiences tidal flows. The computational effort required for 3D modeling of multiple tide cycles is prohibitively time consuming, so certain times during the tide cycle must be chosen for simulation in the 3D model. The flow behavior determined during the previous 2D study was examined to select the times which featured the most extreme flow behavior near the scour hole. Steady-state simulations of those most extreme flood and ebb conditions are the most likely to cause growth of the existing scour hole, and those times were chosen for the 3D simulations.

Using the 2D solution, the flow velocity at a location in the scour hole was extracted to determine when the maximum velocity occurred during flood and ebb tides. However, the velocity magnitudes during the flood tides were often larger than the velocity magnitudes during the ebb tides; therefore, the flow direction was used to distinguish if the extracted velocity magnitude occurred during flood or ebb tide. These velocity magnitudes were then separated to differentiate between the tide cycles. The maximum velocity magnitudes that occurred during flood and ebb tide are shown in Figure 6 and Figure 7, respectively. The green dot in Figure 6 shows the flow condition chosen for the flood tide simulation, and the orange dot in Figure 7 shows the flow condition chosen for the ebb tide simulation. The flood condition corresponds to the flow behavior on January 20, 2019, at 11:00 Greenwich Mean Time (GMT), and the ebb condition corresponds to the flow behavior on January 21, 2019, at 17:00 GMT.

Figure 6. Ocean City model flood velocity magnitudes in main scour hole.

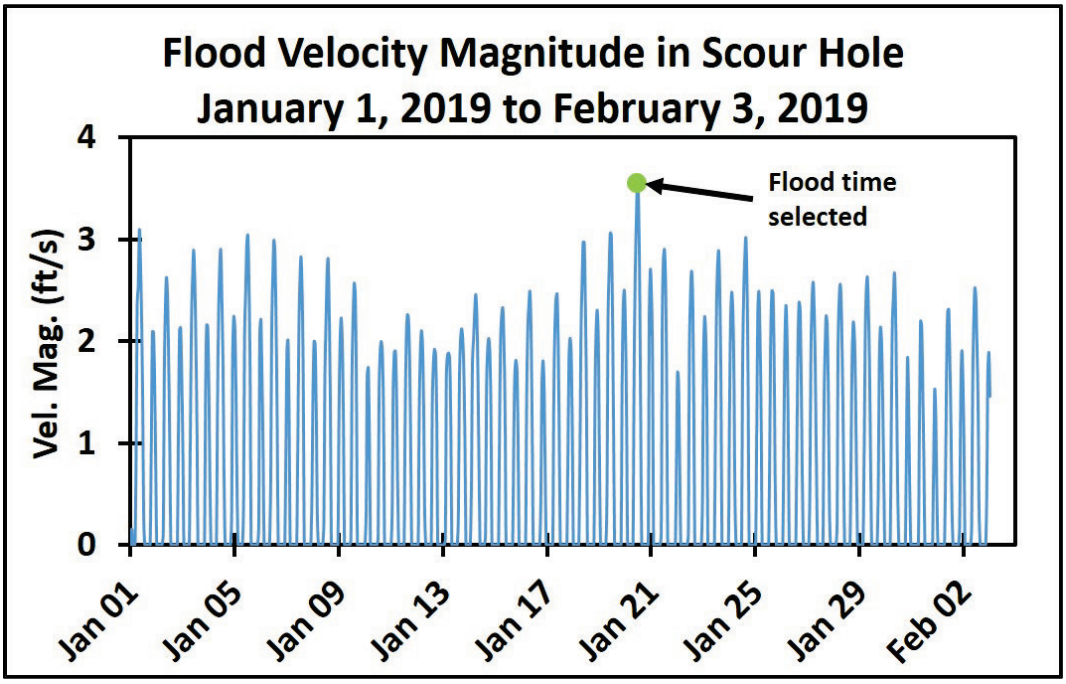

Figure 7. Ocean City model ebb velocity magnitudes in main scour hole.

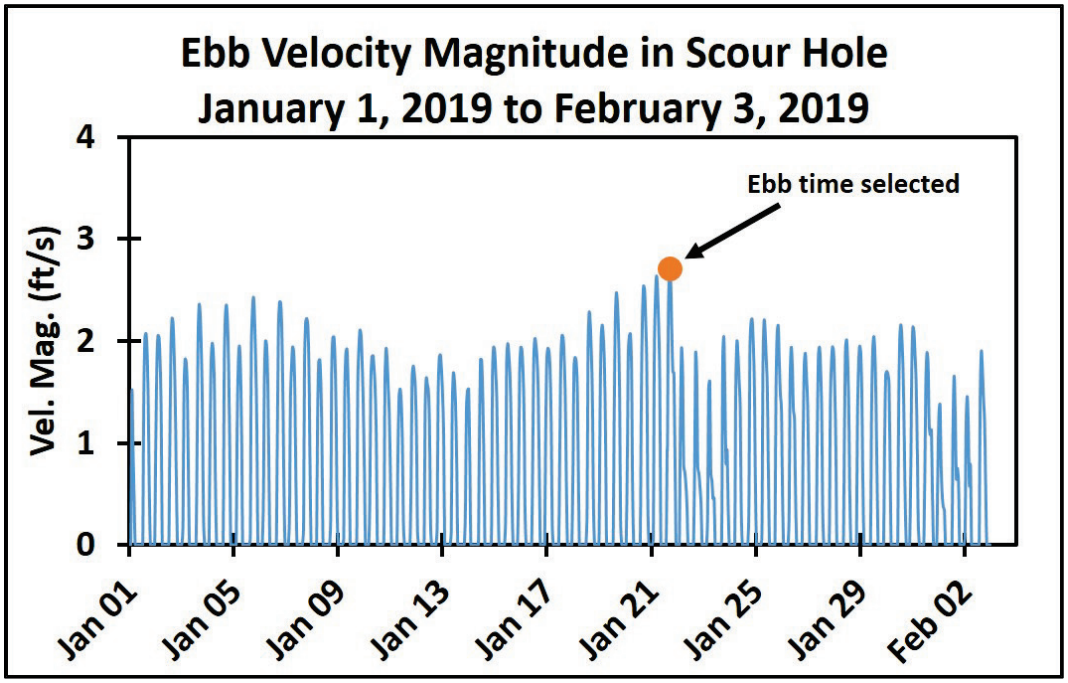

The flux boundaries must be located sufficiently far from the scour hole so that the method of specifying the boundary conditions does not impact the flow solution at the scour hole. The shape of the boundaries was determined using the 2D velocity field once a decision was made regarding how far from the scour hole the inflow and boundaries would be. Contour plots showing the flow depths for the flood and ebb tides are shown in Figure 8 and Figure 9, respectively. The gray coloring in these figures represents areas of the 2D domain that are dry. For the flood tide flow condition, the entire channel near the scour hole is submerged. However, for the ebb tide flow condition, the water level drops, and the center of the channel is above water and two channels (one to the east and one to the west) form. Streamlines of the 2D flow for the ebb condition show that the flow behavior in each channel is independent of the other channel. Therefore, since the scour hole is located in the western channel, the flow domain for the ebb flow condition includes only the western channel.

In the area of Isle of Wight Bay containing the scour hole, the flow enters the flow domain from one end of the bay (either the north or south end) and exits at the opposite end for both the flood and ebb conditions. The flow behavior and size of the bay in this area is conducive to using only two flux boundaries in the model — one inflow and one outflow. The flux boundaries are oriented such that the flow velocity at each flux boundary — both inflow and outflow — is perpendicular to the boundary. Each flux boundary must also not be located such that flow both enters and exits that boundary at any time during the simulation. This condition means that the flux boundaries should not pass through any eddies. Figure 8 and Figure 9 show the flow patterns from the 2D study for the flood and ebb conditions chosen for this 3D study. The black lines indicate the flow streamlines from the 2D study. The streamlines that are generally circular, such as those in the top left, top right, and bottom right of the Figure 8, indicate the presence of eddies. These eddies limit the possible locations for the flux boundaries. Eddies are also present in the time of the most extreme ebb flow (Figure 9). Figure 10 and Figure 11 show the flux boundary locations selected for the flood and ebb simulations, respectively.

Figure 8. 2D Model flow depths and streamlines — flood condition.

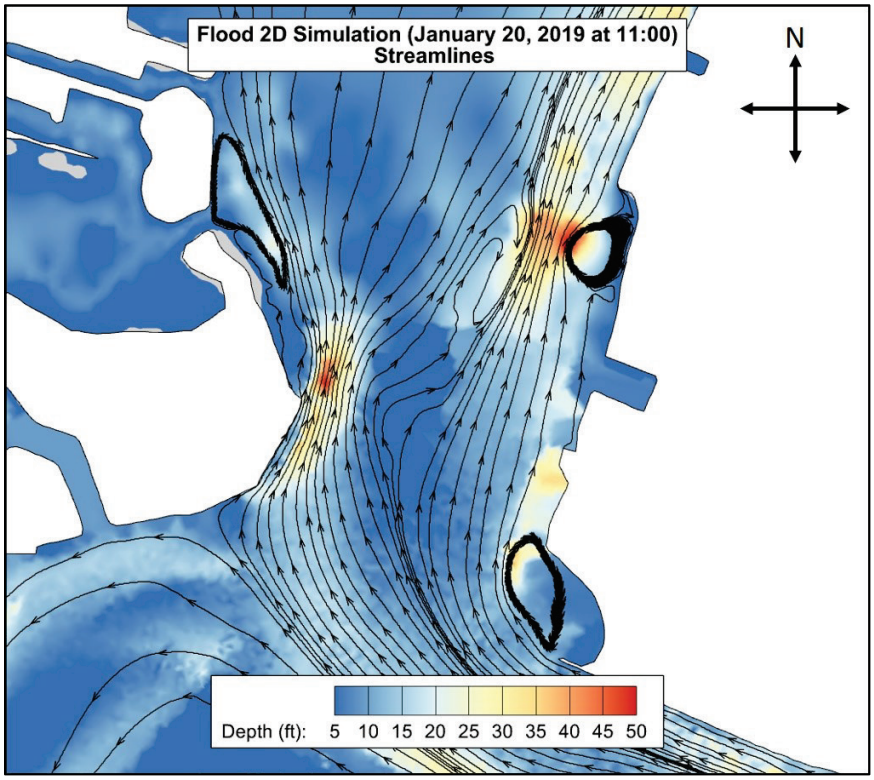

Figure 9. 2D Model flow depths and streamlines — ebb condition.

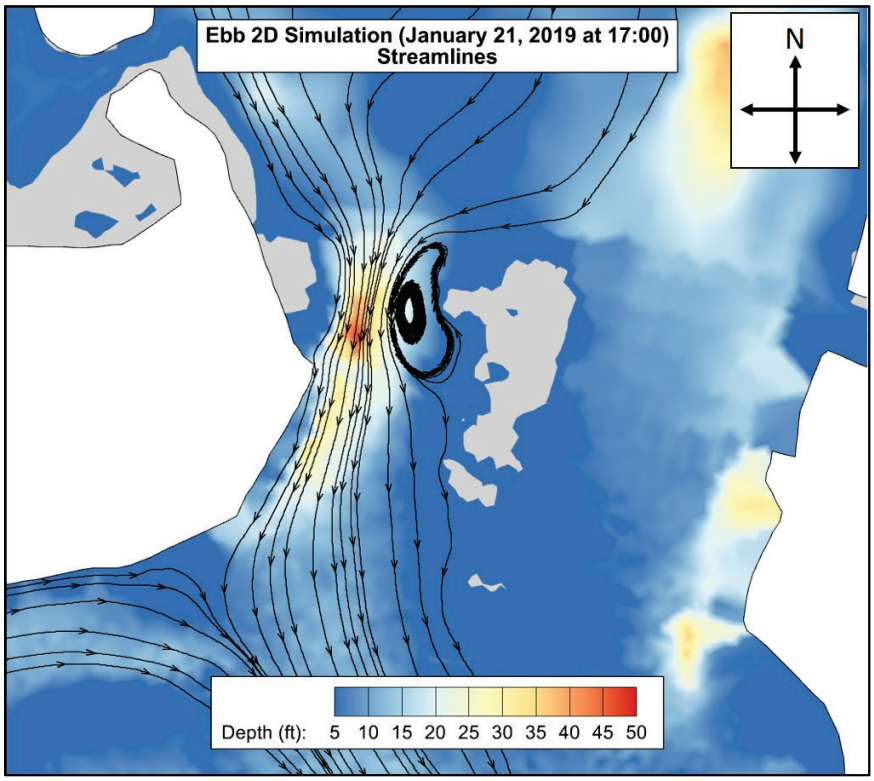

Figure 10. 3D flow domain flux boundaries — flood condition.

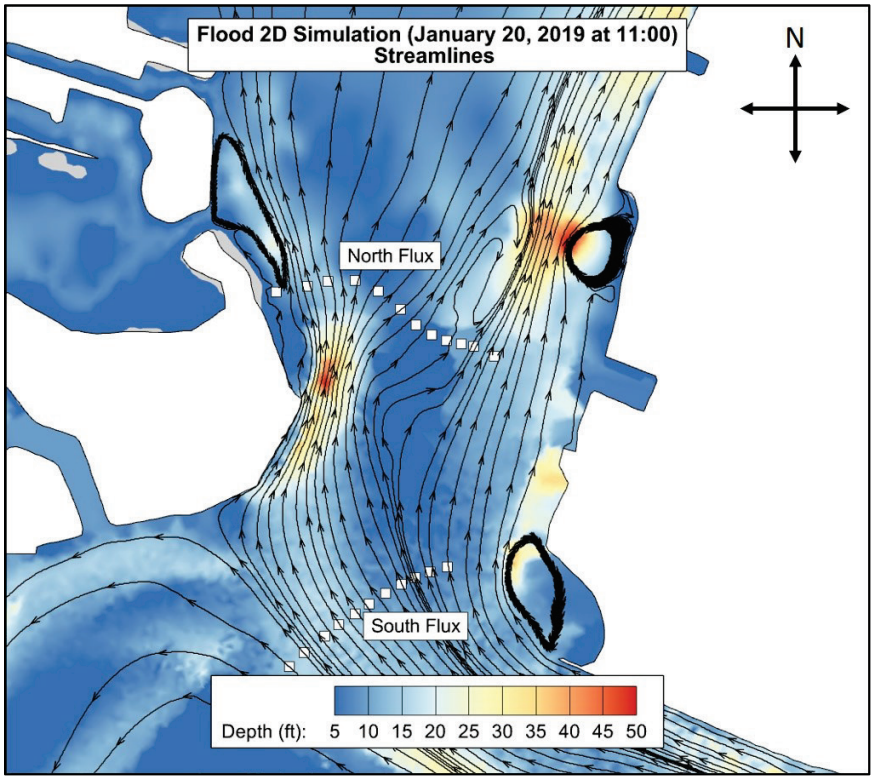

Figure 11. 3D flow domain flux boundaries — ebb condition.

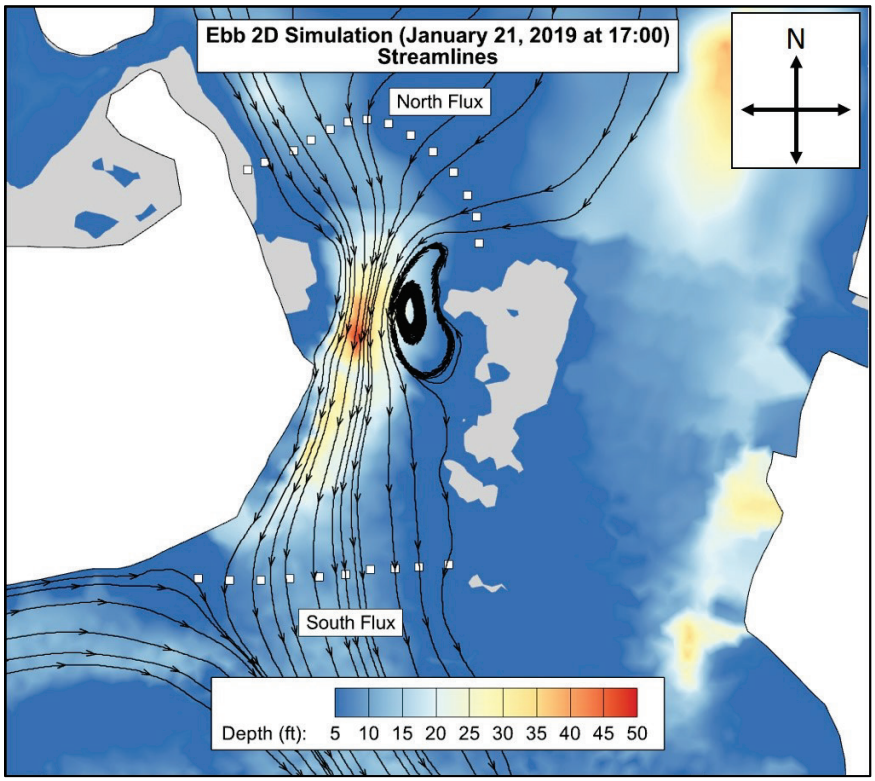

3.1.5 Sides

During the 2D simulation, areas of the flow domain could change from wet to dry depending on the flow conditions. RANS-AdH does not have such wetting-and-drying capabilities, so the flow domain must be restricted to areas that remain submerged throughout the simulation. Thus, the 3D mesh can be referred to as an all-water mesh. In shallow areas of a flow domain, mesh quality requirements dictate that smaller elements are used, which significantly increases the size of the mesh in those areas. Therefore, some very shallow areas of the 2D flow domain may need to be removed during the creation of the 3D flow domains. The nearshore and beach impacts are sufficiently captured by the 2D from which the flow inputs for this 3D study have been obtained.[1]

The all-water requirement and shallow water area mesh size considerations collectively require that the 3D flow domain cannot extend across the entire channel included in the 2D simulations — particularly because of shoaling that is present in the center of the channel. The choice of which streamlines to use and what depth to use as the lower limit of the flow domain is determined from a combination of engineering judgement/modeler experience and testing different mesh sizes and depth limits.

These side boundaries coincide either with streamlines of the 2D flow solution or with the contour of the depth threshold chosen. Streamline locations are chosen because the side boundaries will be treated as walls during the simulation, and by definition, there is no flow across a streamline. Placing the boundaries along streamlines ensures that the location of the sides of the flow domain will not significantly affect the flow solution. The depth limit is chosen either because the region is so shallow that the flow velocity in the corresponding areas is very small or because the region is far from the area of interest for the simulation and including it in the flow domain is unnecessary. After the locations of the flow domain sides are chosen, vertical surfaces are created to ensure that the flow domain is enclosed.

[1] C. Jared McKnight, Tate O. McAlpin, Keaton E. Jones, and Cassandra G. Ross. In preparation. *Ocean City Inlet, Maryland: A Two Dimensional Shallow Water Adaptive Hydraulics (AdH-SW2D) Hydrodynamic and Sediment Transport Model*. ERDC/CHL Technical Report. Vicksburg, MS: US Army Engineer Research and Development Center.

Aligning a side boundary with a streamline dictates only the shape of that boundary based on where the streamlines intersect the inflow boundary. The locations of the side boundaries must be considered carefully because the side boundaries are not physically present in Isle of Wight Bay and are only created for the sake of the model. Therefore, the side boundaries must not be placed close enough to the areas of interest of the study that these boundaries significantly affect the flow behavior in the areas of interest.

The locations of the side boundaries of the flood condition flow domain were chosen by creating streamlines at different locations along the inflow boundary and observing how closely the observed streamline approached the area of interest. Two streamlines were selected using the following criteria: the streamline must neither pass too closely to the area of interest nor too far from the area of interest (to produce a reasonably small mesh). The side boundaries for the flood domain are shown in Figure 12.

Figure 12. 3D domain side boundary locations — flood condition.

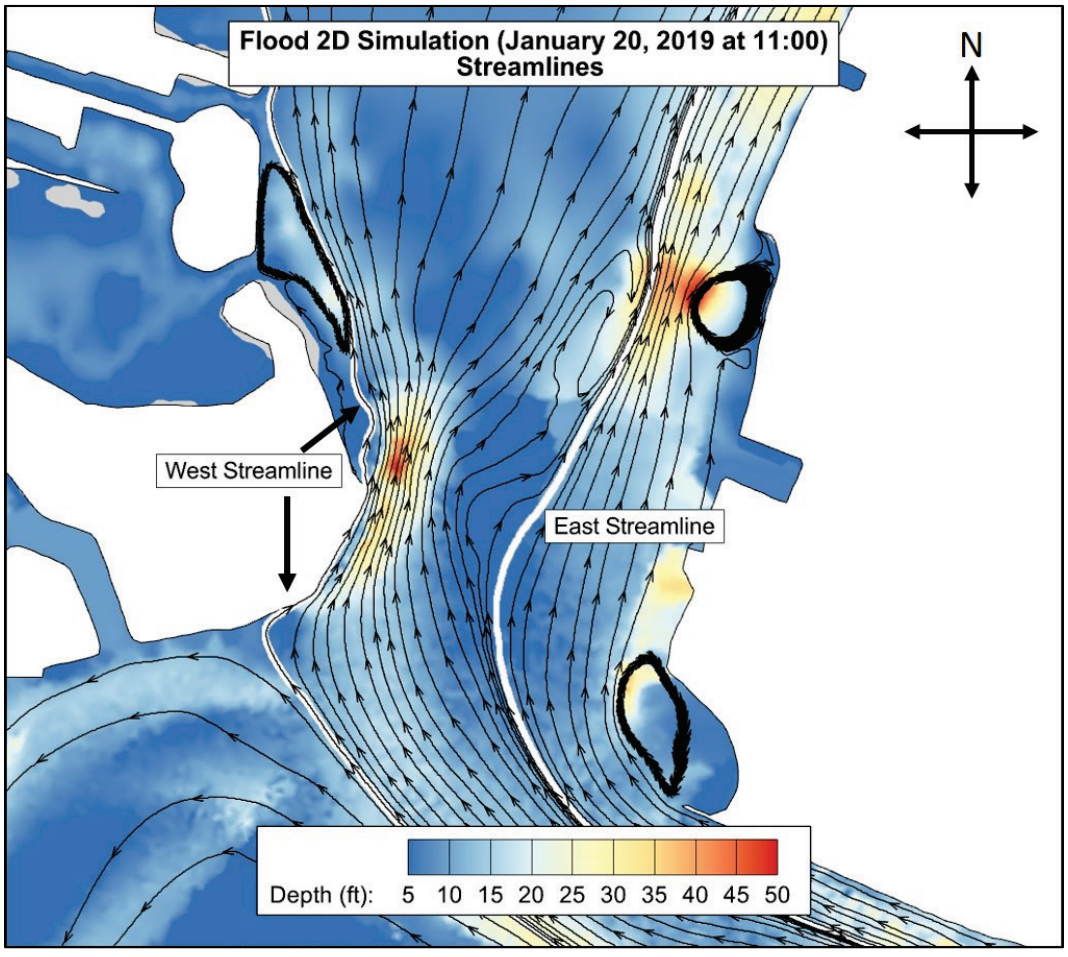

For the ebb flow condition, the flow depths are lower than for the flood flow condition, so the side boundary locations were chosen from the flow depths. The side boundaries are a combination of the 3 ft depth contours of the 2D flow solution and the boundary of the 2D flow domain. A 3 ft depth contour was chosen because the magnitude of the flow velocity in areas with depths below that level are small (velocity magnitudes average approximately 0.5 ft/s in the northeast bound area removed). The locations of the side boundaries for the ebb simulations are shown (dotted white boundary lines) in Figure 13.

Figure 13. 3D domain side boundary locations — ebb condition.

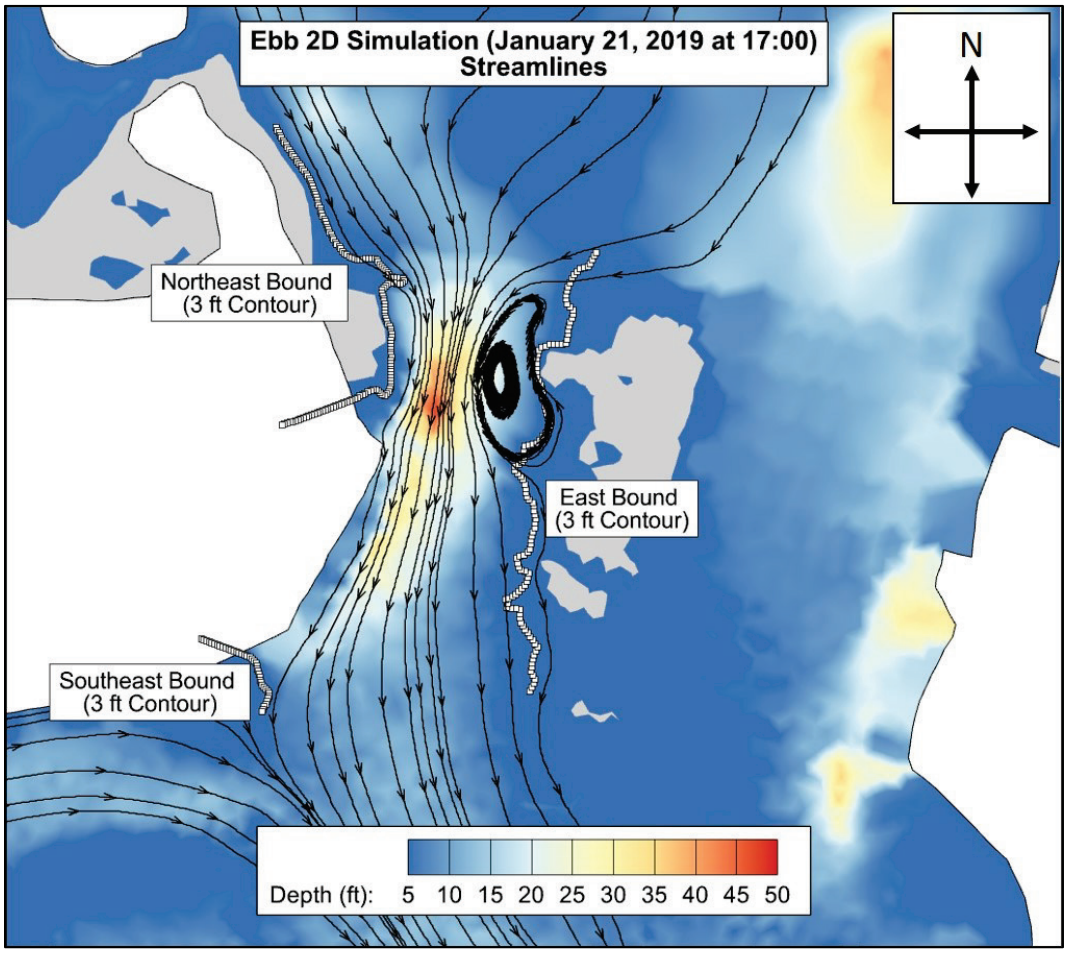

3.1.6 Total flow domain summary

Each portion of the flood and ebb flow domains has been described in detail. The flow domain consists of a bottom (the bathymetry), two flux boundaries (an inflow boundary at the upstream end and an outflow boundary at the downstream end), and two side boundaries (one to the east and one to the west). Combining the flux boundary locations with the side boundary locations defined the planwise extents of the flow domains for both flow conditions simulated during this study (Figure 14 and Figure 15). The flow domain for the flood condition (shown in Figure 16) is approximately 1,800 ft (north to south) by 700 ft (east to west). The flow domain for the ebb condition (shown in Figure 17) is approximately 1,300 ft (north to south) by 400 ft (east to west).

Figure 14. 3D flow domain extents — flood condition.

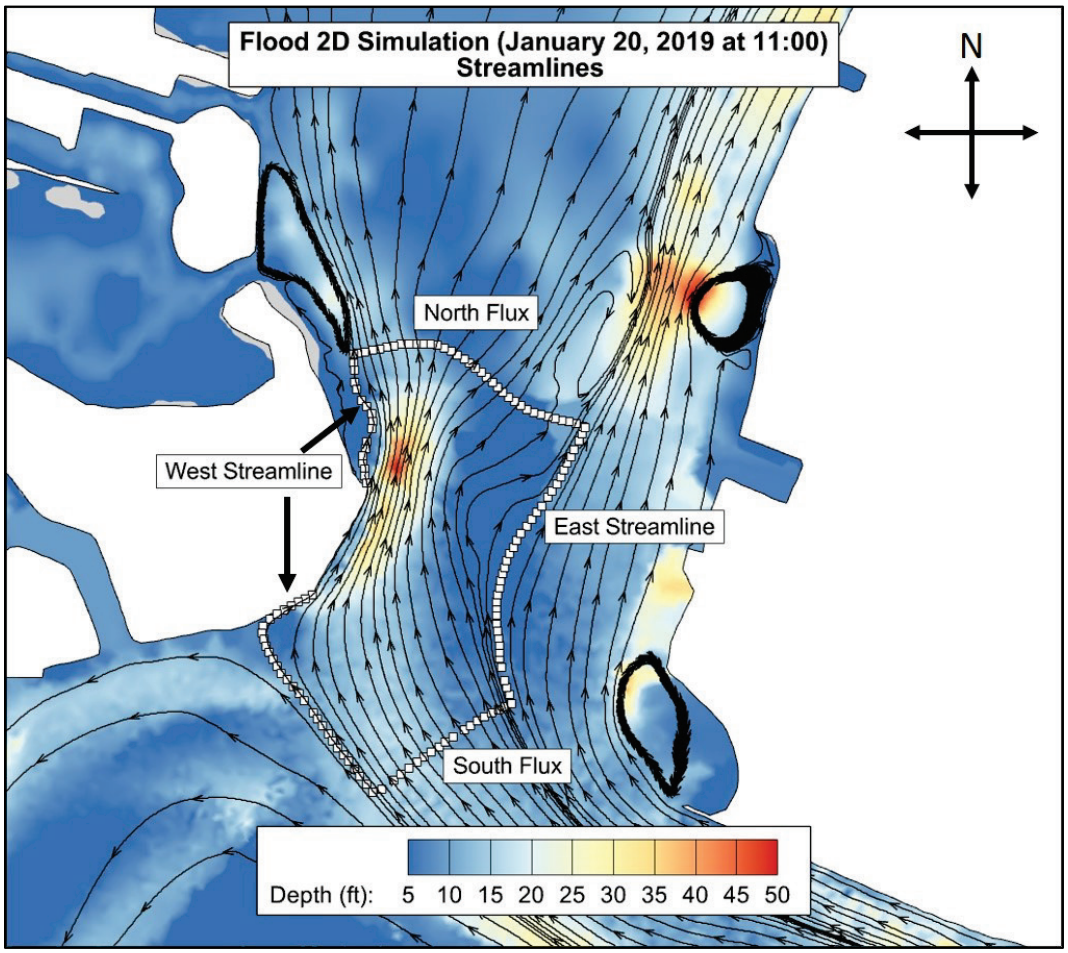

Figure 15. 3D flow domain extents — ebb condition.

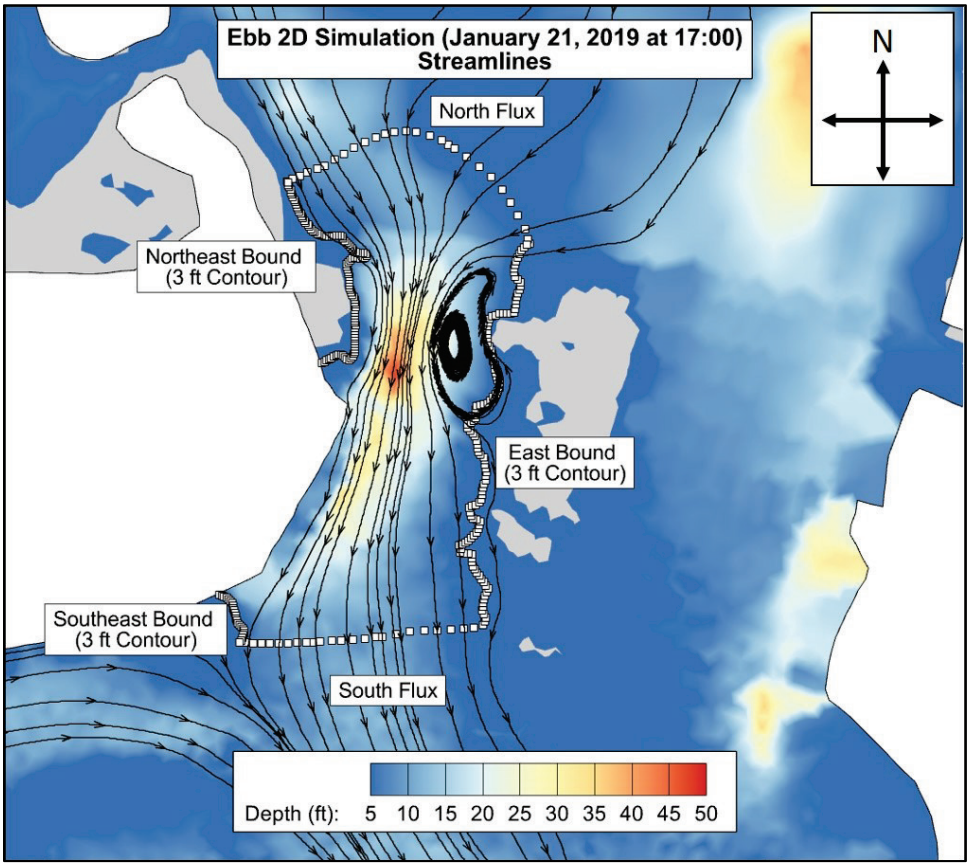

Figure 16. Flood domain extents shown on an aerial view image.

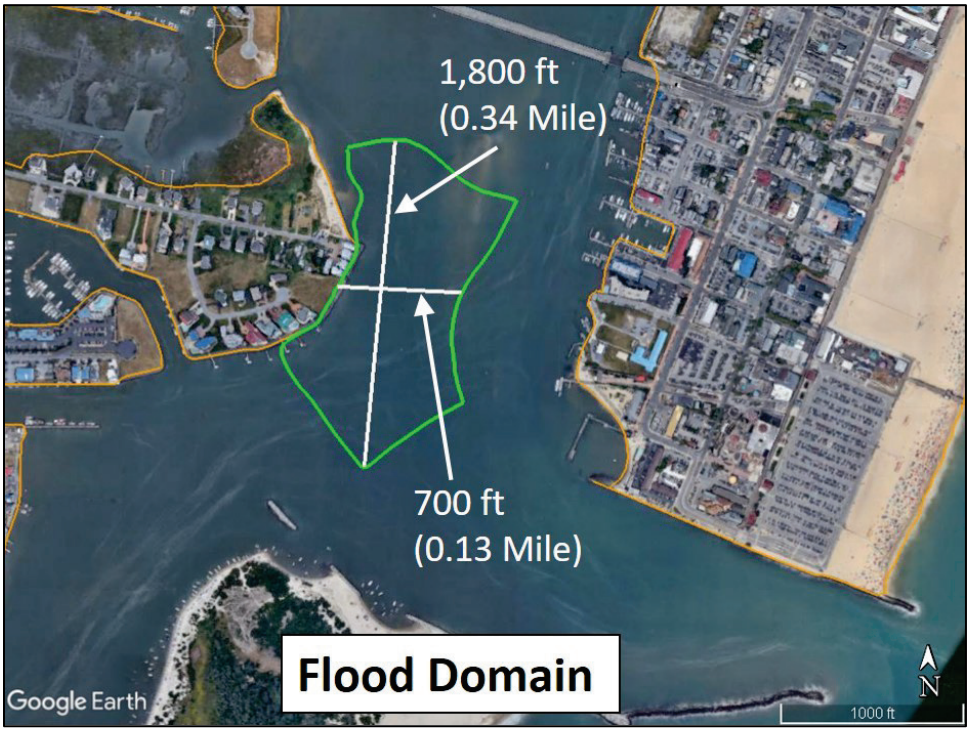

Figure 17. Ebb domain extents shown on an aerial view image.

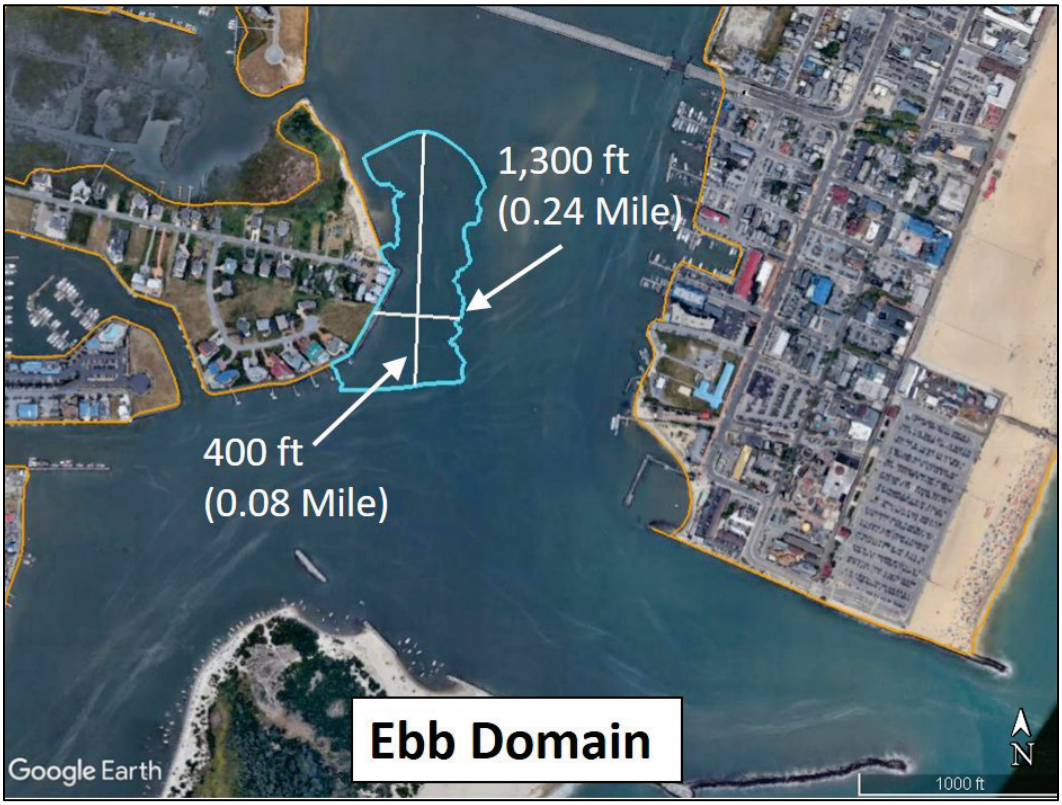

4 Meshing

Once the flow domains have been developed (see Chapter 3), it must be discretized into a computational mesh. The general idea behind creating a mesh for a RANS-AdH simulation is to accurately capture the shape of the boundary faces and have a sufficient amount of resolution to get a reasonable flow solution. A mesh that meets those two criteria is sufficient because the automatic mesh adaption capabilities in RANS-AdH can be used to adjust the mesh to more accurately calculate the details of the flow during a simulation. The lengths of the sides of mesh elements required for a 3D simulation are generally much smaller than those of a 2D simulation of the same planwise area. To illustrate that difference in mesh element sizes, Figure 18 shows the 2D mesh that is used as a starting point for the 3D geometry development. The top image shows the entire 2D flow domain, while the middle and bottom images show zoomed-in views of that mesh. The bottom image also includes the planwise extents of the flood and ebb 3D flow domains. The bottom image provides an indication of how much smaller the mesh elements in the 3D meshes will be than the 2D mesh.

Figure 18. 2D mesh and 3D flow domain extents (green – flood domain; blue – ebb domain).

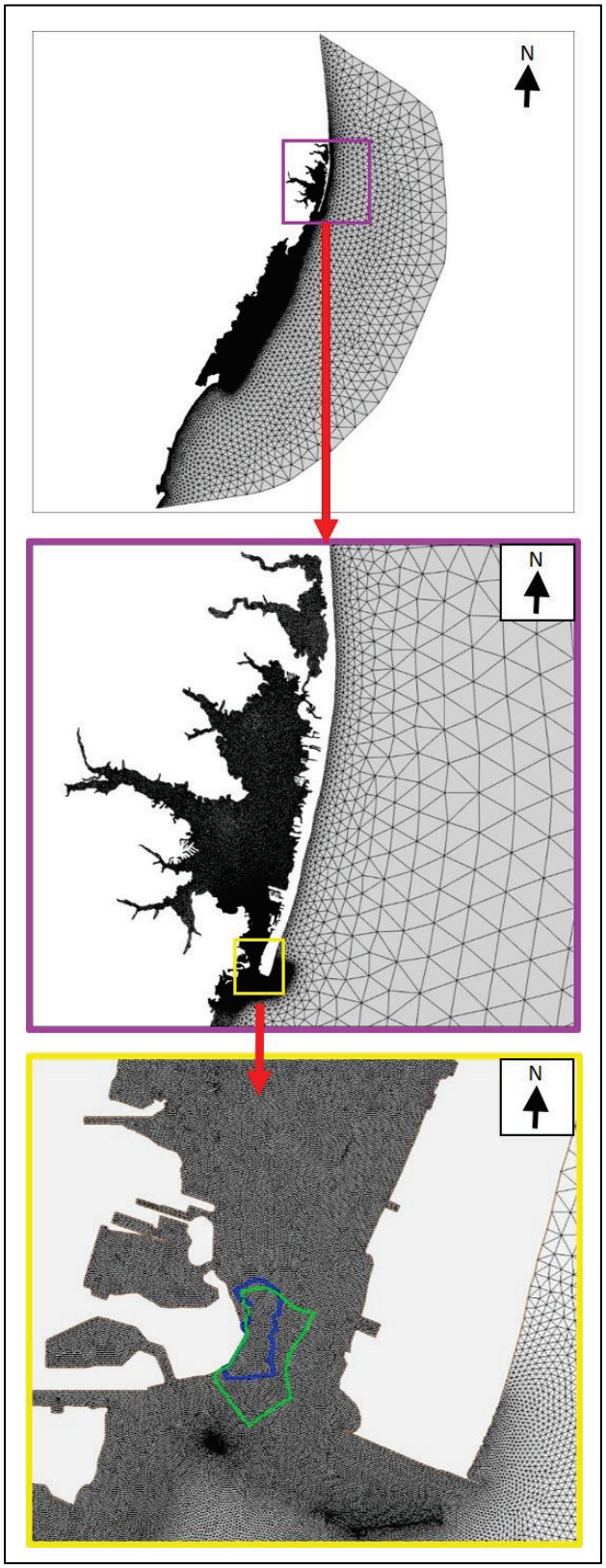

4.1 General meshing challenges

A major challenge of this study was creating meshes that captured the geometric detail in the flow domain but did not have so many nodes and elements that completing the simulations exceeded the available computational resources. RANS-AdH simulations require tetrahedra-only meshes, and the tetrahedra must have a low aspect ratio to ensure that the element quality is high enough to produce accurate flow solutions. Shallow areas of the flow domain require significantly higher refinement for adequate mesh resolution and quality. A large area near the scour hole that is shallow relative to the remainder of the flow domain requires a disproportionately large amount of the nodes and elements in the mesh. The flow domain was divided into three regions (Figure 19 and Figure 20). One region was defined so that a different roughness value could be applied to match the 2D solution (Body 2 in Figure 19 and Figure 20). The purpose of defining the other two regions was to separate shallow areas (Body 3) and deeper areas (Body 1) so that they could have different size parameters for meshing. Sufficiently resolving the mesh in the shallow area while retaining a total mesh element count that is not computationally prohibitive (~10 million volume elements using HPC resources), is the primary challenge of creating the 3D meshes.

Figure 19. Flood flow domain meshing divisions.

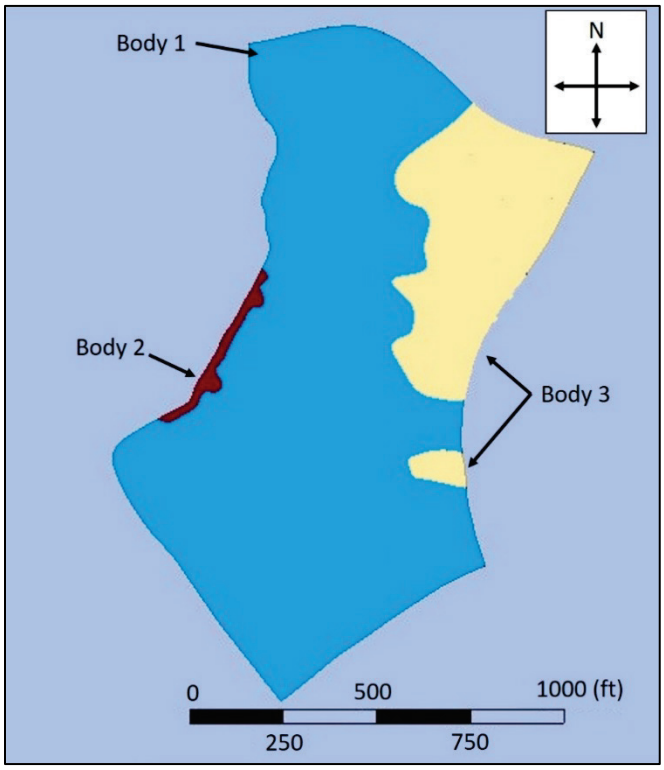

Figure 20. Ebb flow domain meshing divisions.

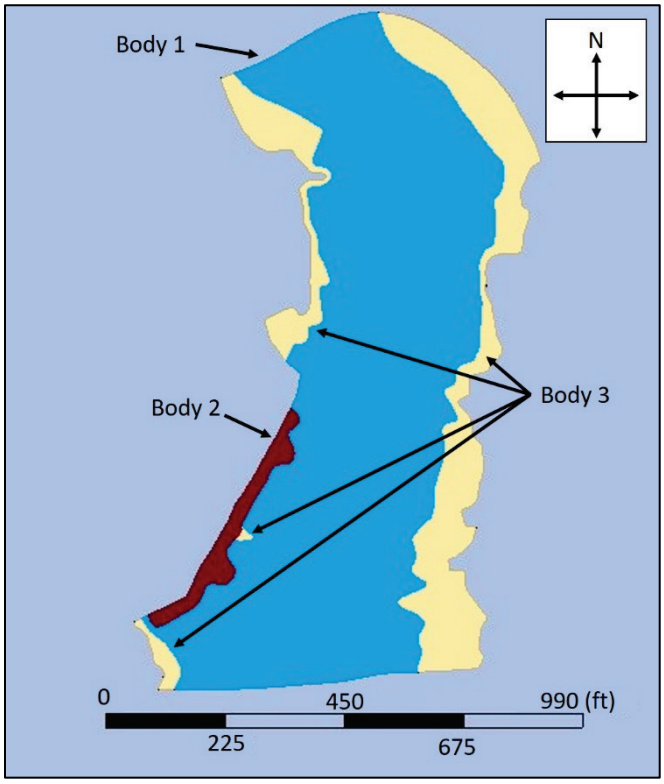

4.2 Meshing procedure

To address the challenge posed by the large variation of depth in the flow domain (and to separate areas of the bathymetry for different material properties), the flow domain was divided into three areas. Specifically, separating the flow domain into different pieces allowed for smaller element sizes to be specified for the shallow areas of the mesh and for larger elements to be created in the deeper areas of the mesh. Each mesh was generated iteratively by choosing mesh sizes for the different regions and generating the corresponding meshes to determine the mesh and element count for the entire mesh. If either the mesh resolution or total node and element count results were insufficient, adjustments were made to the size parameters, and the flow domain was remeshed. Such iterations continued until a sufficient mesh had been created.

4.3 Final meshes

The flood condition mesh has 8,036,224 volume elements and 1,740,576 nodes. The lengths of the elements ranged from 0.4 to 2.0 ft. At the scour hole, the element sides are approximately 0.5 to 1.6 ft long. The ebb condition mesh has 8,338,682 volume elements and 1,599,832 nodes. The

lengths of the elements ranged from 0.2 to 0.7 ft. At the scour hole, the element sides are approximately 0.3 to 0.7 ft long. The amount of mesh refinement throughout the mesh is sufficient for RANS-AdH to generate an appropriately detailed solution for mesh adaption to be used to provide the additional mesh refinement necessary for a mesh independent flow solution. The total element count for each mesh is below the element count upper limit for a reasonable simulation. Since both meshes satisfy both the refinement and total element count criteria, these meshes were used for all the flood and ebb condition simulations.

Images of the flood condition and ebb condition meshes are shown in Figure 21 and Figure 22, respectively. These images show the planwise variation in the element size throughout the flow domain. Figure 23 and Figure 24 show the mesh resolution near the scour hole. The total element count for the different regions as a percentage of the total element count for the flood and ebb meshes is shown graphically in Figure 25 and Figure 26, respectively. A summary of the element numbers for each of the three divisions of the flood and ebb meshes is shown in Table 1 and Table 2, respectively. For the flood domain, the shallow area (Body 3) comprises only 15% of the total flow domain volume, but sufficiently resolving that region in the computational mesh required 44% of all mesh elements. As a comparison, Body 1 contains almost 84% of the flow domain volume but contains only 55% of the volume elements in the mesh. For the ebb domain, the shallow area (Body 3) comprises 7% of the total flow domain volume but sufficiently refining that region in the computational mesh required 61% of all mesh elements.

Figure 21. Flood simulation bed mesh resolution.

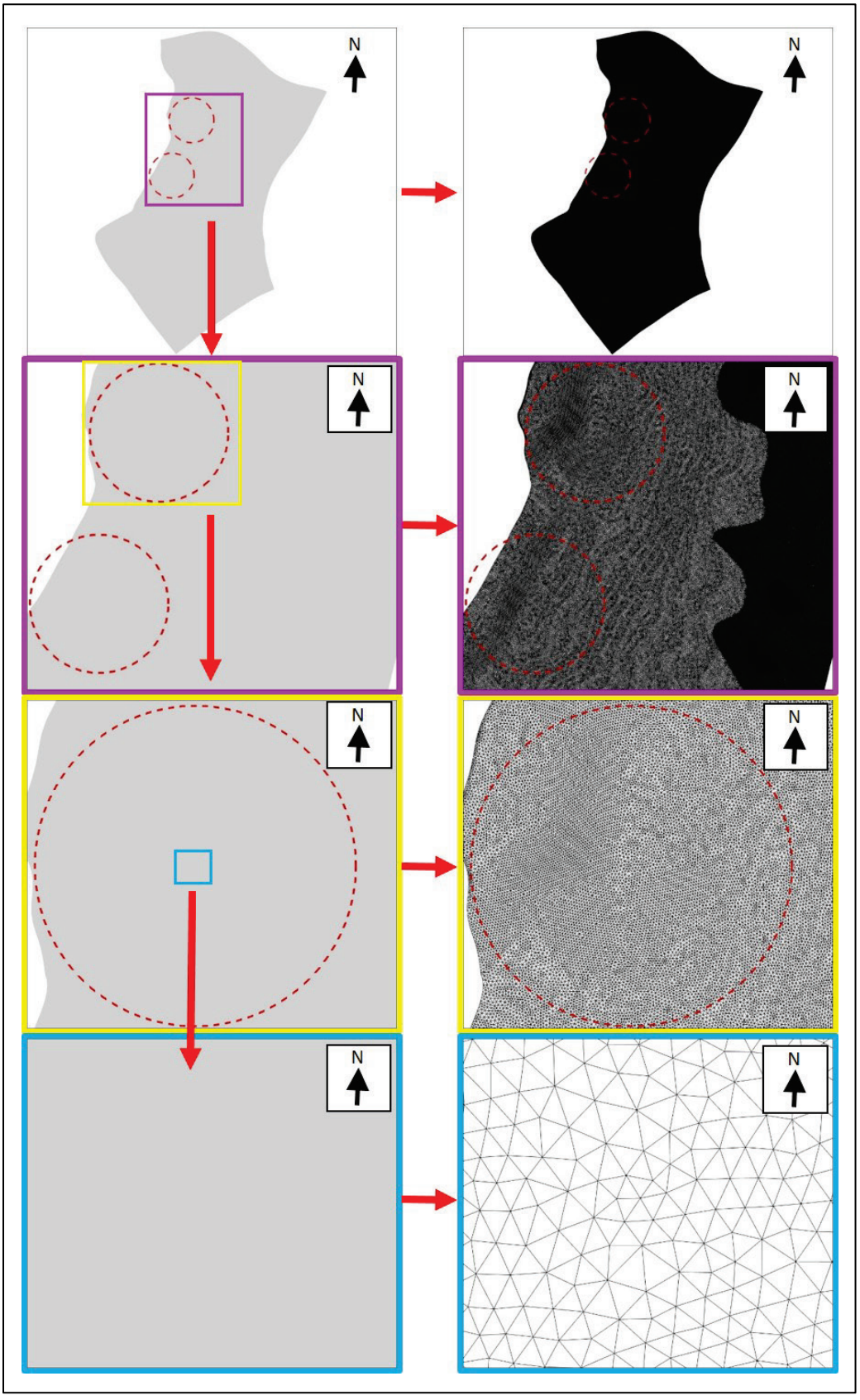

Figure 22. Ebb simulation bed mesh resolution.

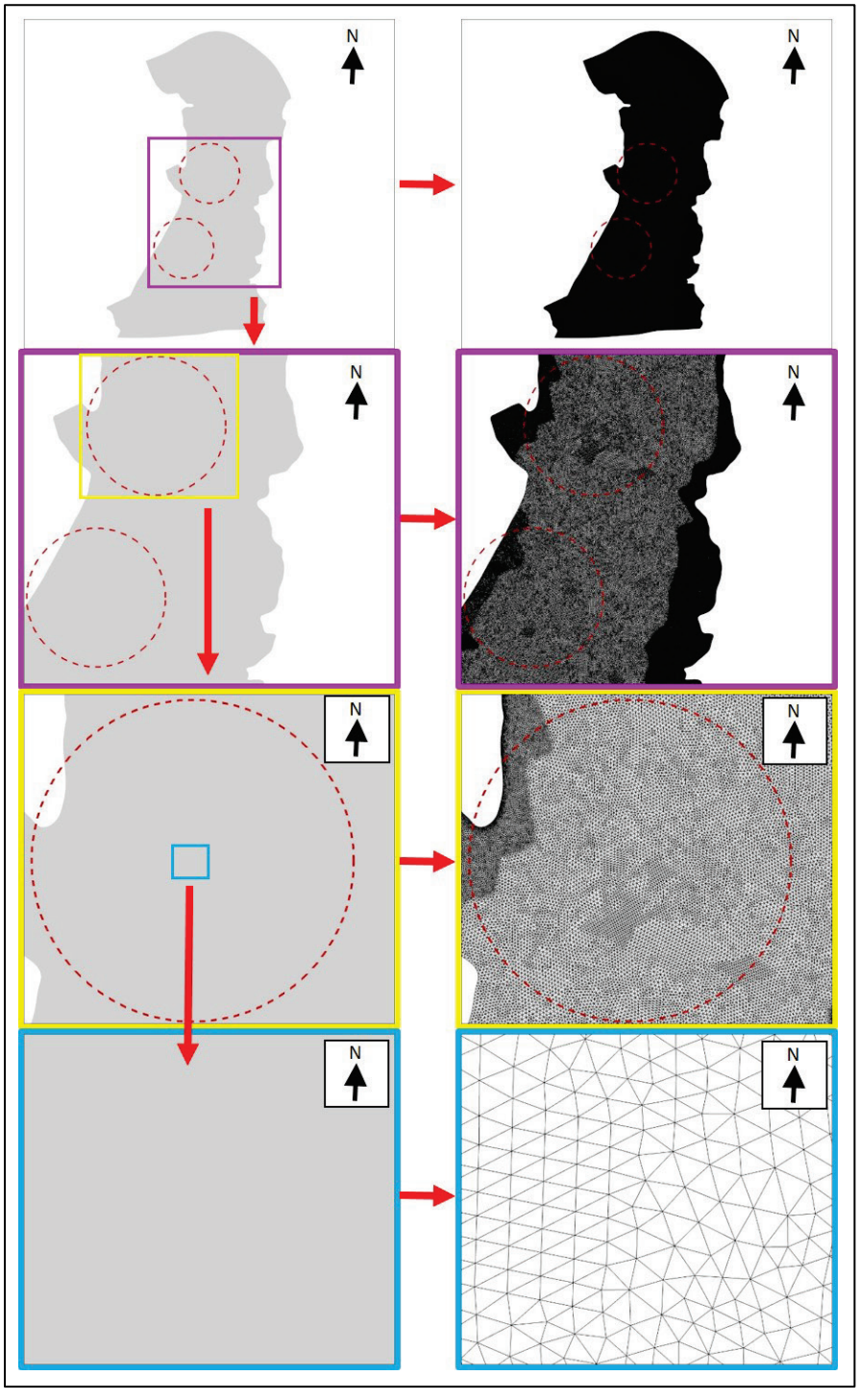

Figure 23. Vertical resolution — flood mesh.

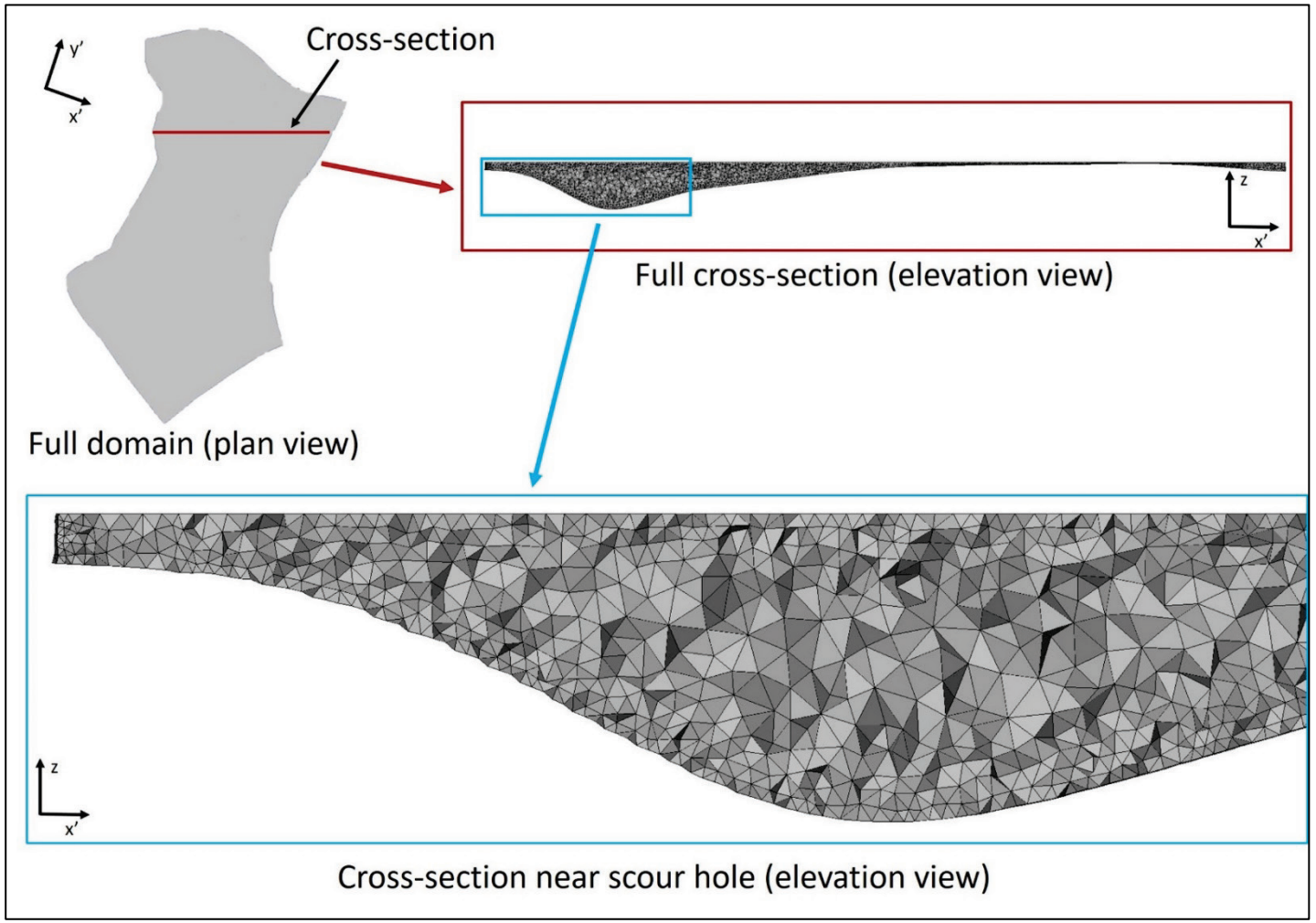

Figure 24. Vertical resolution — ebb mesh.

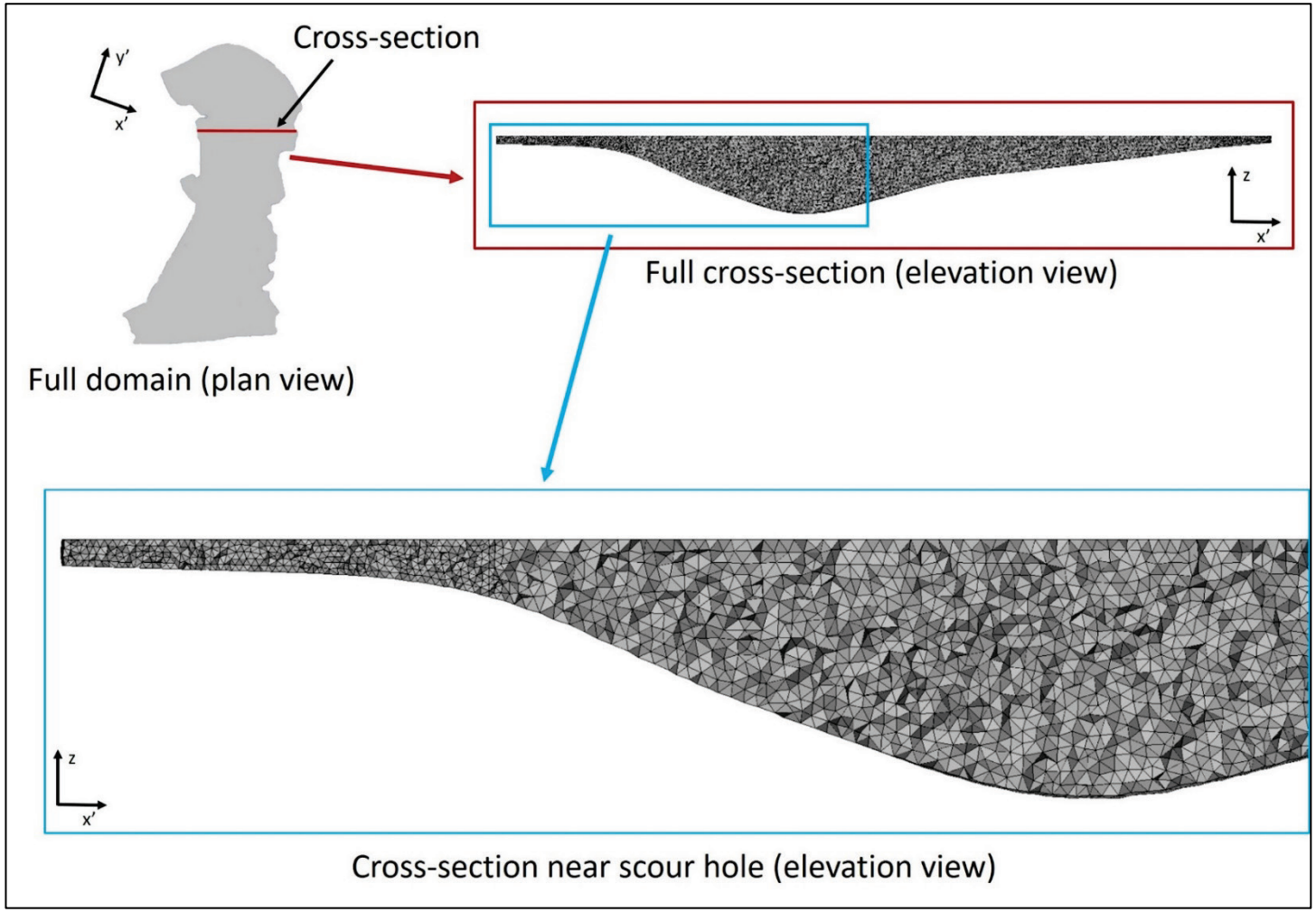

Figure 25. Flood mesh element breakdown.

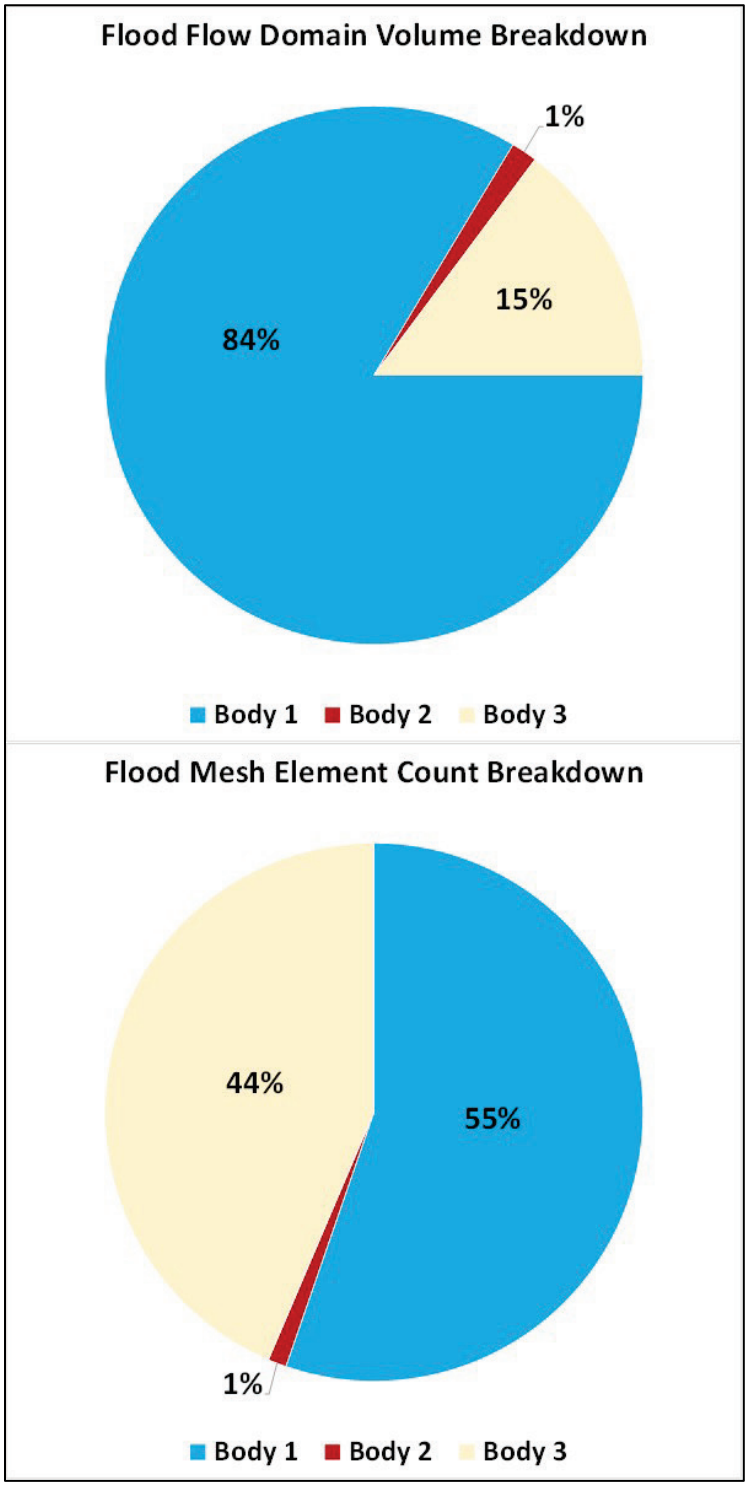

Figure 26. Ebb mesh element breakdown.

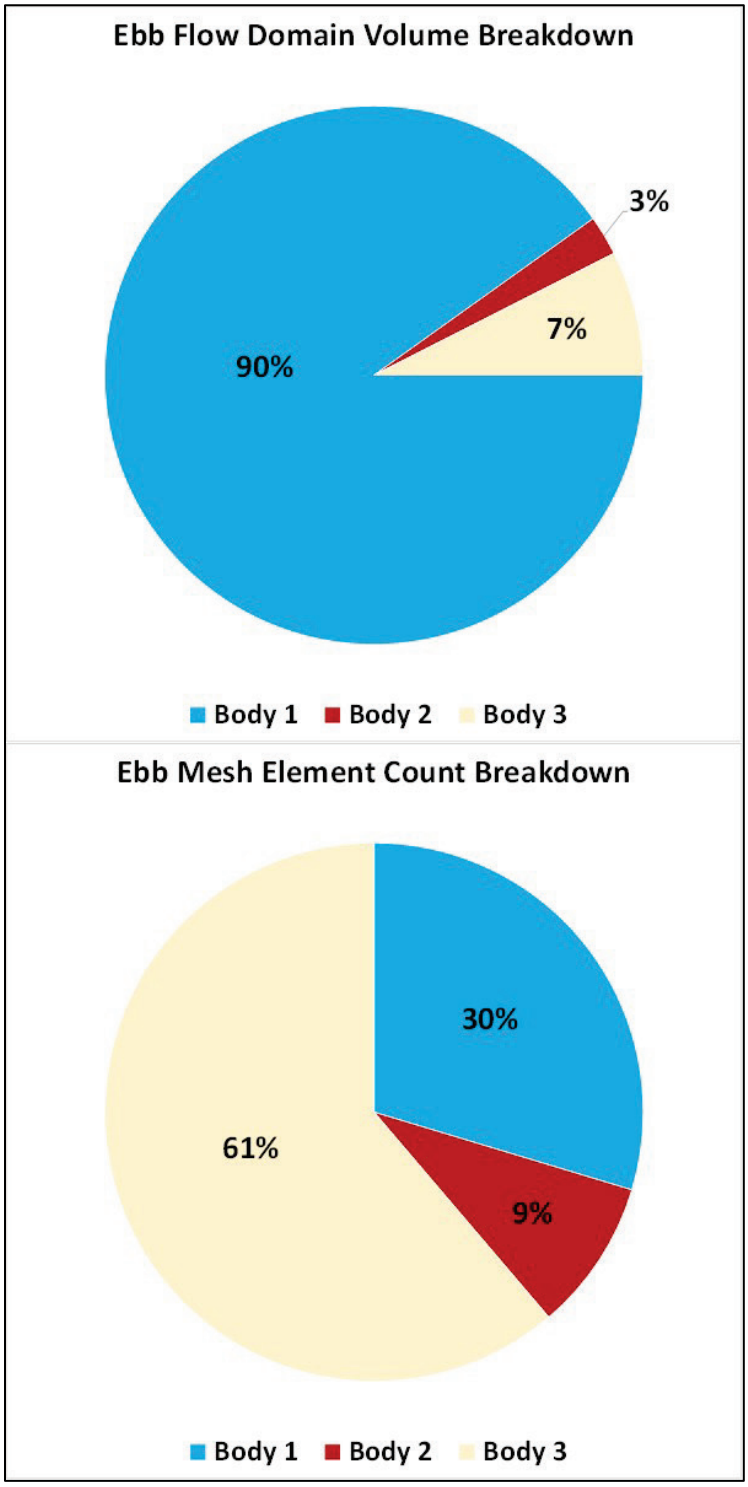

Table 1. Element count versus area — flood mesh.

Geometry	Volume (ft^3)	Portion of Total Mesh Volume (%)	Element Count	Portion of Total Mesh Element Count (%)
Body 1	11,951	84	4,444,774	55
Body 2	224	1	88,959	1
Body 3	2,114	15	3,502,491	44
Total	**14,289**	**100**	**8,036,224**	**100**

Table 2. Element count versus area — ebb mesh.

Geometry	Volume (ft^3)	Portion of Total Mesh Volume (%)	Element Count	Portion of Total Mesh Element Count (%)
Body 1	6,688,206	90	2,473,203	30
Body 2	177,796	3	759,235	9
Body 3	554,829	7	5,106,244	61
Total	**7,420,832**	**100**	**8,338,682**	**100**

5 Boundary Conditions and Simulation Procedure

In this chapter, the boundary conditions will be discussed. Each flow domain contains two flux boundaries — one inflow and one outflow (as discussed in Chapter 3). The method for specifying the flow on these boundaries is discussed in detail. Each flow domain has several no-flux boundaries, and how these boundaries are treated during each simulation is discussed. Finally, the general simulation setup, including how automatic mesh adaption was employed, is included in this chapter.

5.1 Boundary Conditions

The boundary conditions for both the flood and ebb simulations correspond directly to the 2D simulation input and results.

5.1.1 Inflow

For each simulation, the discharge through the model was defined as a series of velocities along the inflow boundary. For each inflow boundary node, the velocity was determined by interpolating the 2D velocity solution at the location of the node. The vertical (z-coordinate) velocity for each inflow node is set to zero. This method of assigning the velocity at the inflow ensured that the appropriate discharge was used for each simulation. Using depth-averaged velocities on the inflow boundary causes some distortion of the flow behavior in the 3D results. Therefore, the results near the inflow boundary must be disregarded when evaluating the results of the 3D simulations.

5.1.2 Outflow

A hydrostatic pressure boundary condition was applied to the surface elements on the outflow boundary. The top edge of the outflow boundary corresponds to the water surface elevation from the 2D simulation. The nodes that lie on that edge are assigned a pressure of zero, and every other node on the outflow boundary is assigned a pressure based on a hydrostatic pressure distribution. No direct restriction is placed on the flow velocity at the outflow boundary.

At the inflow boundary, the specified vertical velocity is zero, which does not reflect the actual flow behavior, so the flow solution near the outflow boundary should be disregarded when evaluating the results of the 3D simulations.

5.1.3 Water surface

For the simulations reported in this report, the water surface boundary is treated as a stationary, frictionless wall. The water surface boundary was determined by adding the adding the depth at each node in the 2D solution at the time of interest (separately for both the flood and ebb conditions) to the elevation of that node.

5.1.4 Bathymetry

The bathymetry in both flow domains used in this study is treated as slip boundaries. The affects the bathymetry has on the flow are calculated using a roughness value corresponding to the materials of which the boundary is composed. The bathymetry for both flood and ebb conditions has regions with two different surface roughness values. These regions are shown in Figure 27 and Figure 28. The surface roughness values used in this study are shown in Table 3 and are the same values used in the 2D study. Further information on how these friction values were obtained is contained in the technical report for the 2D study[1].

Table 3. Friction values used for each material.

Zone	Manning's *n*
Material 1	0.025
Material 2	0.035
Sides	0.000

[1] C. Jared McKnight, Tate O. McAlpin, Keaton E. Jones, and Cassandra G. Ross. In preparation. *Ocean City Inlet, Maryland: A Two Dimensional Shallow Water Adaptive Hydraulics (AdH-SW2D) Hydrodynamic and Sediment Transport Model*. ERDC/CHL Technical Report. Vicksburg, MS: US Army Engineer Research and Development Center.

Figure 27. Flood simulation material division.

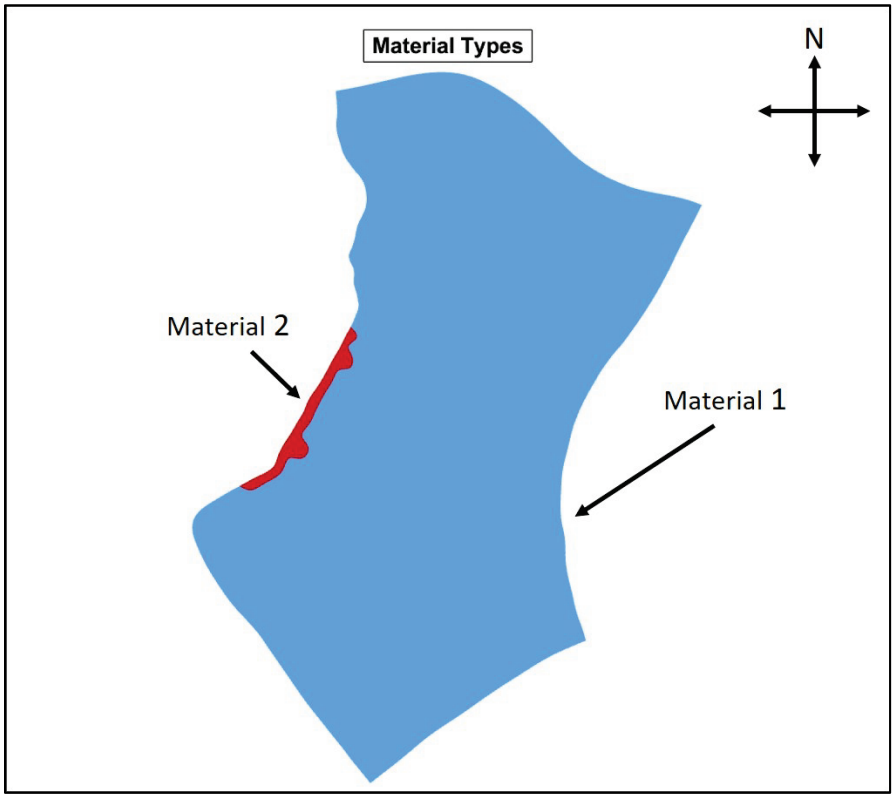

Figure 28. Ebb Simulation material division.

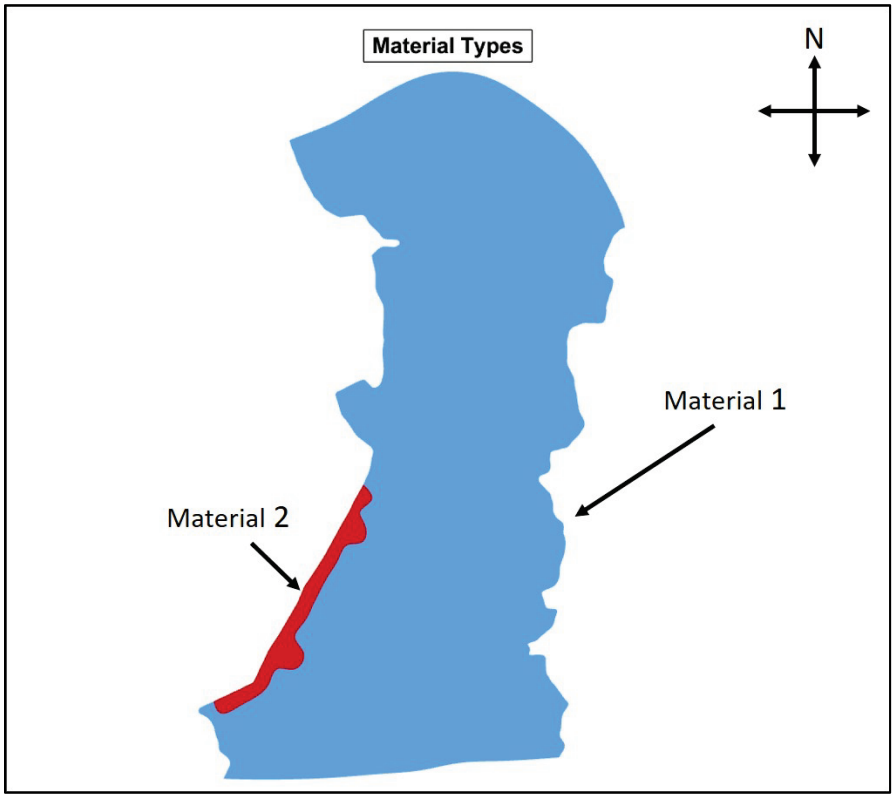

5.2 Simulation procedure summary

The simulation procedure for both flood and ebb models followed the process described in Section 2.2. An eddy viscosity of 0.00001 ft^2/s was used for all steady-state simulation results presented in this report (see Chapter 6). After a steady-state flow field using the final eddy viscosity was obtained, the simulation residual around the scour hole was probed to determine an appropriate mesh adaption threshold to ensure a mesh-independent solution near the scour hole. The mesh refinement tolerance level used was 0.02. One level of adaption was used for all simulations.

The simulations for each flow condition were run on 720 processors on the ERDC Department of Defense Supercomputing Resource Center machine *Jim*. Final results for the flood flow condition required 18 hr of computational time and 13,150 processor hours, and final results of the ebb flow condition required 35 hr of computational time and 39,050 processor hours.

6 Numerical Model Results

In this chapter, the numerical model results of each simulation are presented. Because of the large size of the meshes and the large amount of time required to reach a steady-state condition, the final, steady-state behavior results after mesh adaption had been employed are included.

6.1 Presentation of results

The simulation results are presented as a series of contour plots. These plots show — for both the flood and ebb tide conditions — the flow solution very near the channel bed and at the water surface of the entire flow domain. Further plots are included to show the flow conditions in the two areas of interest. Figure 29 and Figure 30 show the entire planwise flow domain for each simulation with the two areas of interest identified. Plots are included of the flow velocity near the channel bed, at the water surface, and along vertical slices (locations are indicated in Figure 31 and Figure 32). Shear stresses acting on the bed for the entire planwise extents of both the flood and ebb flow domains are also presented.

Figure 29. Areas of Interest for flood simulations.

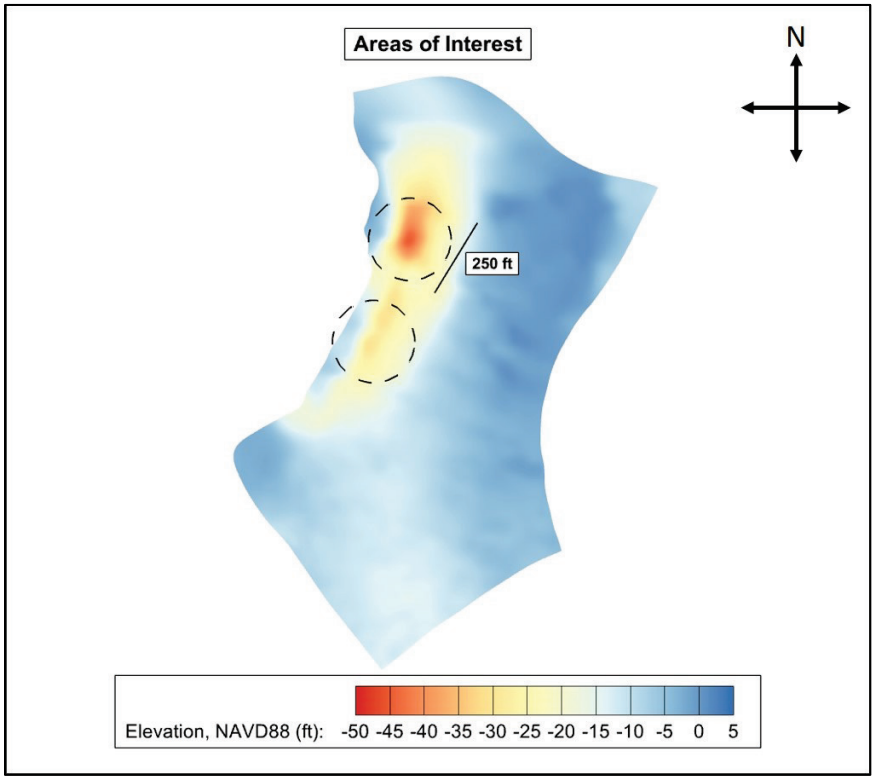

Figure 30. Areas of interest for ebb simulations.

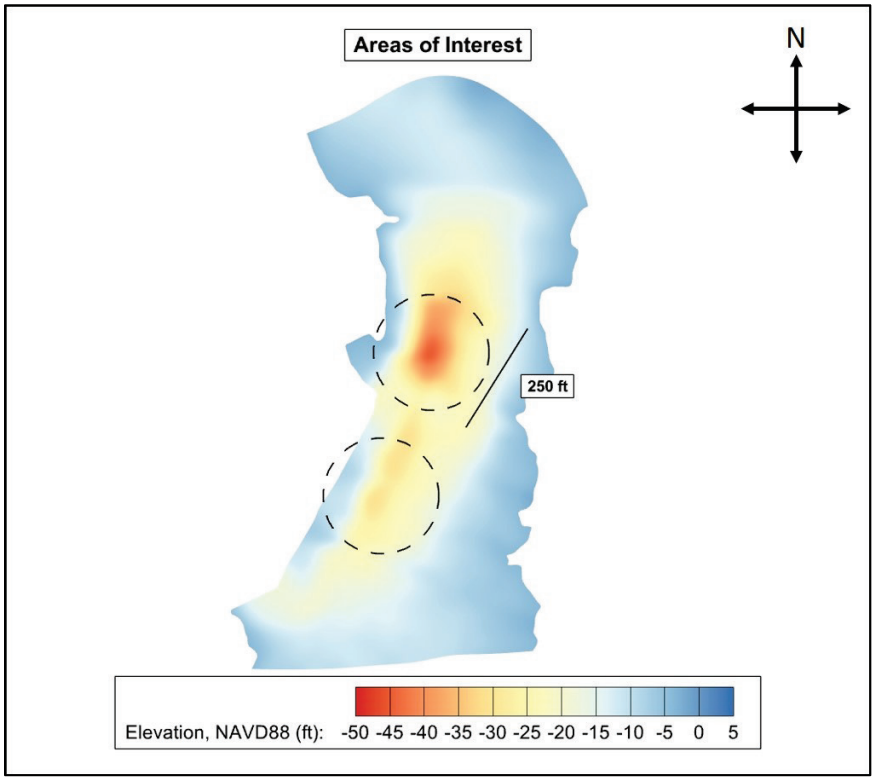

Figure 31. Vertical slice locations for flood condition.

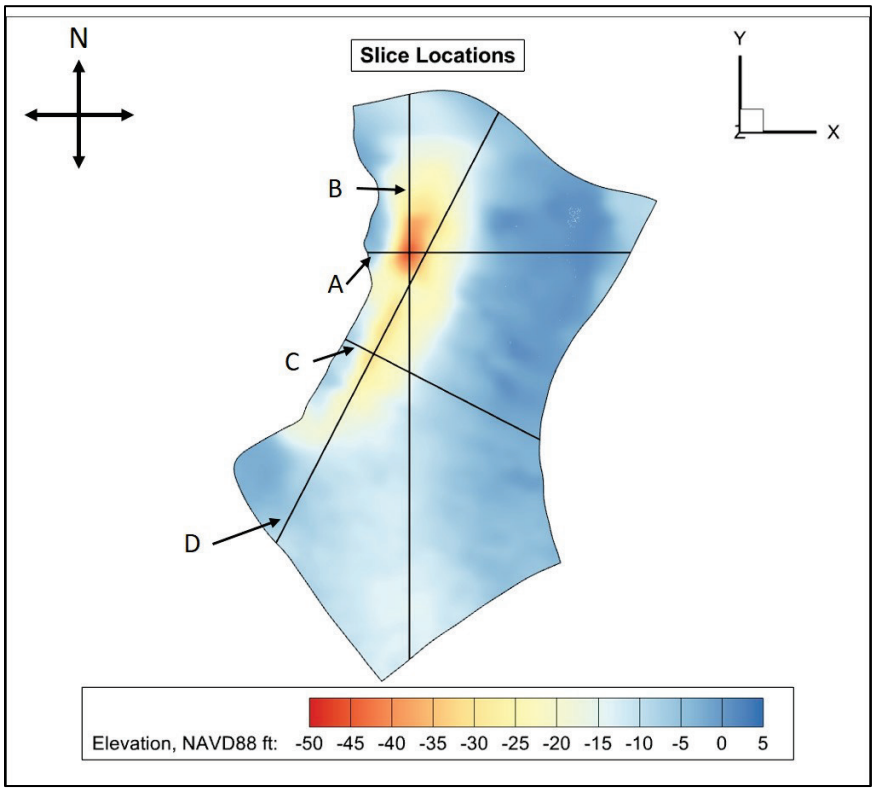

Figure 32. Vertical slice locations for the ebb condition.

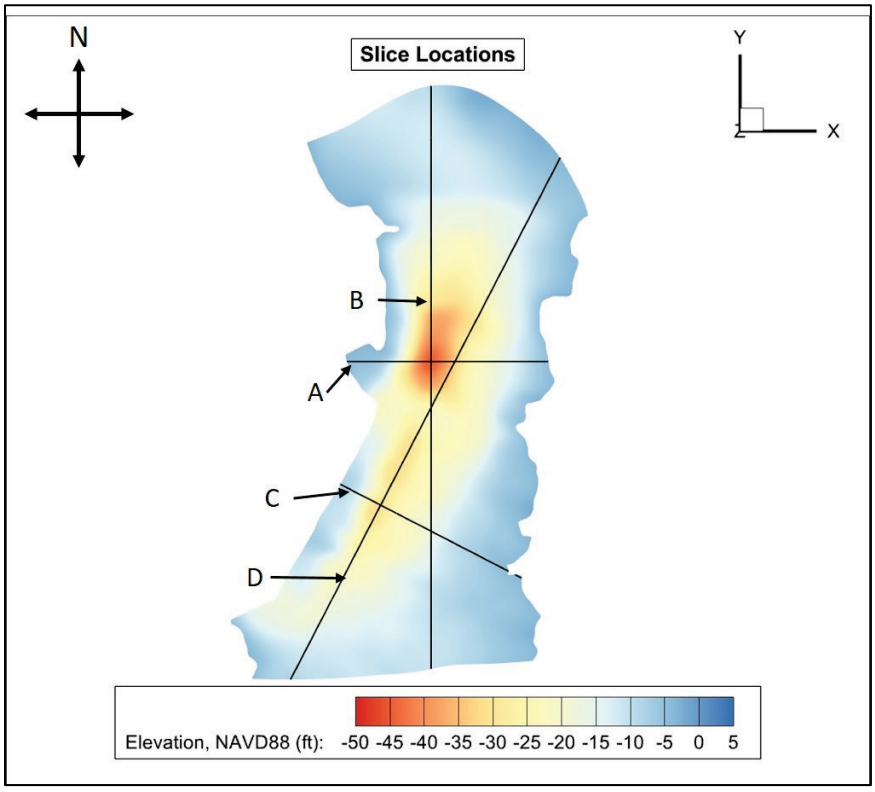

Two quantities are presented: the velocity magnitude and the shear stress acting on the channel bed. The velocity magnitude, V, is defined as

$$V = \sqrt{u^2 + v^2 + w^2} \tag{4}$$

where

u = x-component of flow velocity
v = y-component of flow velocity
w = z-component of flow velocity.

The shear stress τ acting on the channel bed has been calculated as

$$\tau = \frac{1}{2} f \rho V^2 \tag{5}$$

where

f = Darcy's friction factor
ρ = the density of water.

Darcy's friction factor was calculated from the Manning's n values for surface roughness presented in Table 3. The conversion from Manning's n to Darcy's friction factor is

$$f = 8\frac{n^2}{{C_0}^2} gR^{-\frac{1}{3}} \quad (6)$$

where

N = Manning's n
C_o = unit system conversion factory (1.0 for SI units and 1.49 for English units)
g = the acceleration due to gravity
R = a characteristic hydraulic radius.

The characteristic hydraulic radius, R, was taken as the hydraulic radius R_h of the inflow boundary for each mesh, which is defined as

$$R_h = \frac{A}{P} \quad (7)$$

where

A = the surface area of the inflow boundary
P = the perimeter of the inflow boundary.

6.2 Flood flow

6.2.1 Velocity

A contour plot of the velocities "very near" the channel bed for the flood condition is shown in Figure 33. These velocities are said to be very near the bed because the bed in this study if fixed, so the flow velocities at the channel bed are exactly zero. Just above the channel, however, the flow velocities are non-zero, and these are the velocities that are calculated during the simulation and presented in this report. Figure 34 is an enlarged view of the velocity contour plot near the areas of interest. The velocity range shown in the contours is 0–5 ft/s with the blue coloring indicating areas with the smallest velocities and red coloring indicating areas with the largest velocities. The velocities along the inflow (southeastern) boundary should be ignored because these velocities are a consequence of the velocity applied on this boundary having no vertical

variation. The flow is directed generally from the southeast to the north throughout the flow domain. The largest bed velocities are present along the western boundary. The southern area of interest experiences bed velocities up to 5 ft/s whereas the northern area of interest experiences bed velocities up to 4 ft/s. The entire western area of the flow domain experiences much larger bed velocity magnitudes than the eastern two-thirds of the flow channel.

Figure 33. Flood condition bed velocity magnitudes.

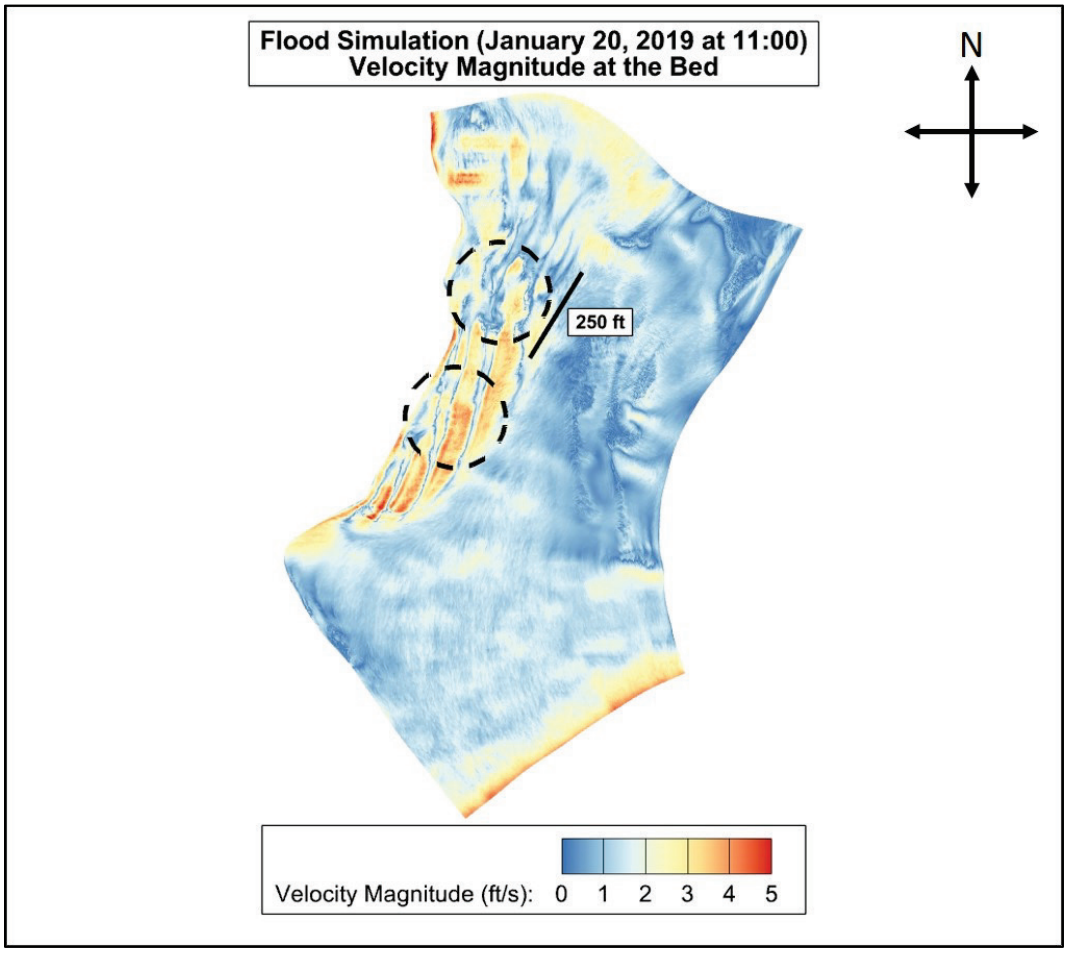

Figure 34. Flood condition bed velocity magnitudes — areas of interest.

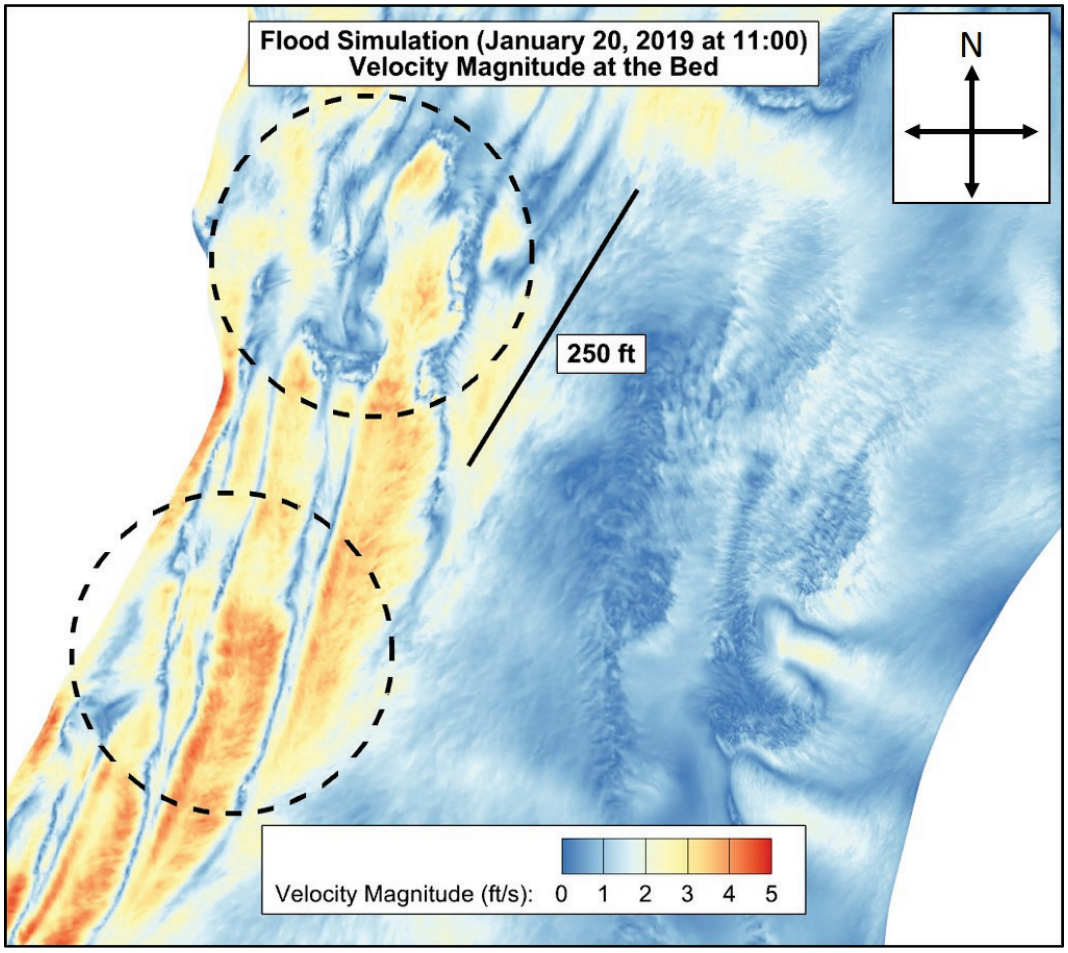

A contour plot of the velocities at the water surface for the flood condition is shown in Figure 35. Figure 36 is an enlarged view of the velocity contour plot for the areas of interest. The velocity range shown in the contours is 08 ft/s with the blue coloring indicating areas with the smallest velocities and red coloring indicating areas with the largest velocities. The velocities along the inflow (southeastern) boundary should be ignored because these velocities are a consequence of the velocity applied on this boundary having no vertical variation. The water surface flow velocity in the northern area of interest ranges from 0 to 8 ft/s, and the southern area of interest experiences water surface velocities of 4 to 8 ft/s.

Figure 35. Flood condition water surface velocity magnitudes.

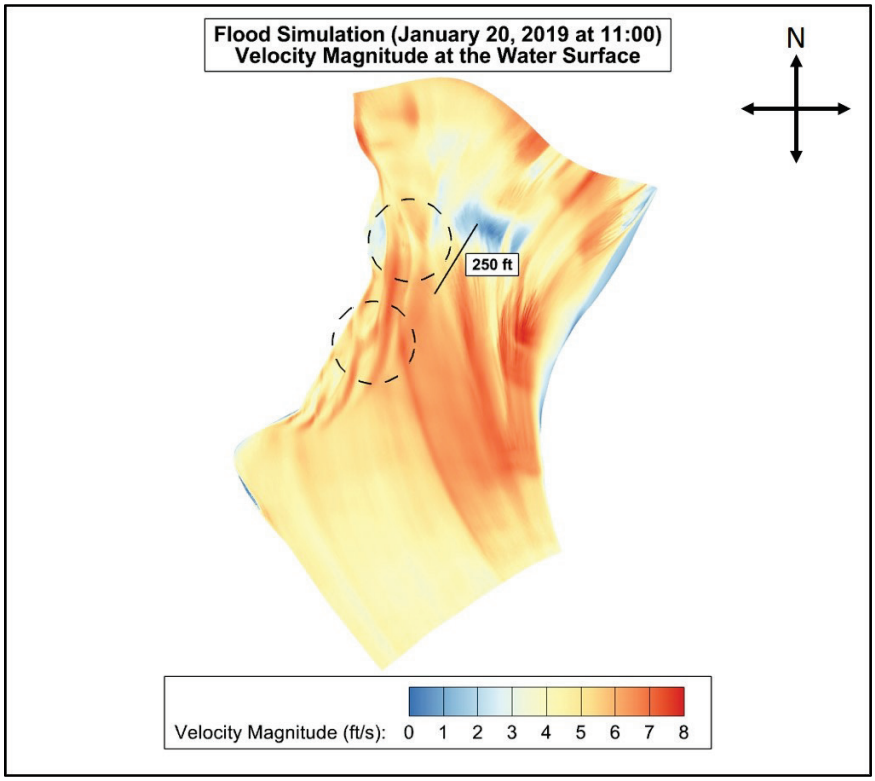

Figure 36. Flood condition water surface velocity magnitudes — areas of interest.

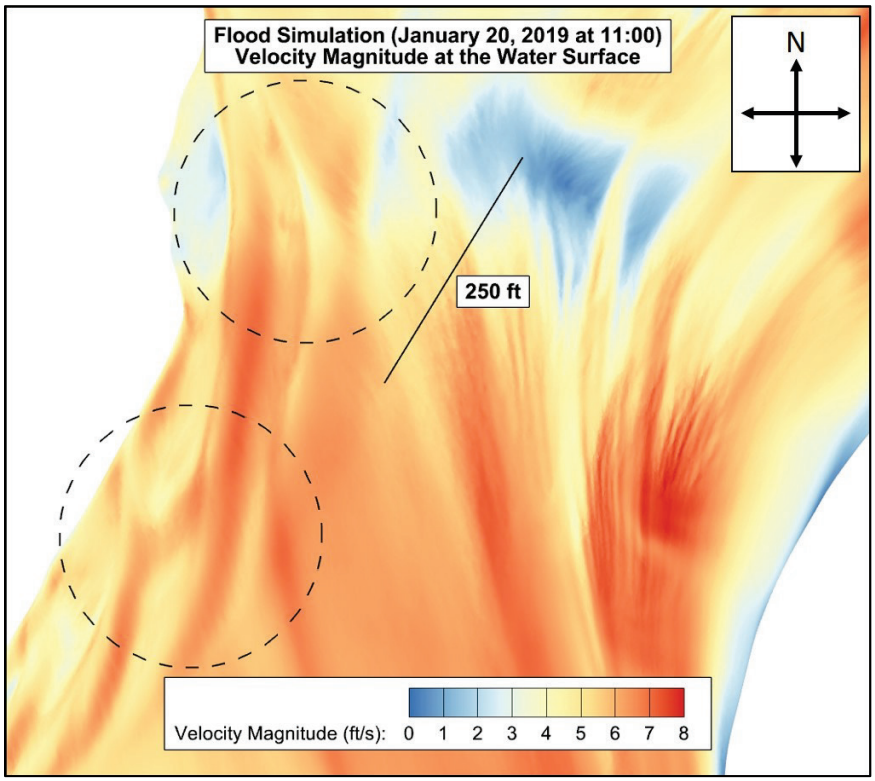

Contour plots showing the velocity distribution along four vertical slices through the areas of interest in the flood domain (see Figure 31) are shown in Figure 37 through Figure 40. The top image in each figure shows the entire slice, and the bottom image is a view of the slice enlarged around one of the areas of interest. The contour range for each plot is 0 to 5 ft/s, with blue coloring indicating velocities near 0 ft/s and the red coloring indicating the velocities near 5 ft/s. The slices through the northern area of interest are shown in Figure 37 (Slice A) and Figure 38 (Slice B). The flow near the area of interest experiences flow velocities of 0 to 5 ft/s. The bottom of the scour hole generally experiences velocities of 0 to 1 ft/s with some areas on the inclines of the scour hole experiencing bed velocities as high as 3 ft/s. In regions to the east of the area of interest (to the right in Figure 37), the velocities are much lower (0 to 3 ft/s) throughout the entire water column. The slices through the southern area of interest are shown in Figure 39 (Slice C) and Figure 40 (Slice D). The velocities in the southern area of interest range from 2 to 5 ft/s. Near the channel bed, the velocity ranges from 2 to 4 ft/s.

Figure 37. Flood simulation velocity magnitude at vertical Slice A.

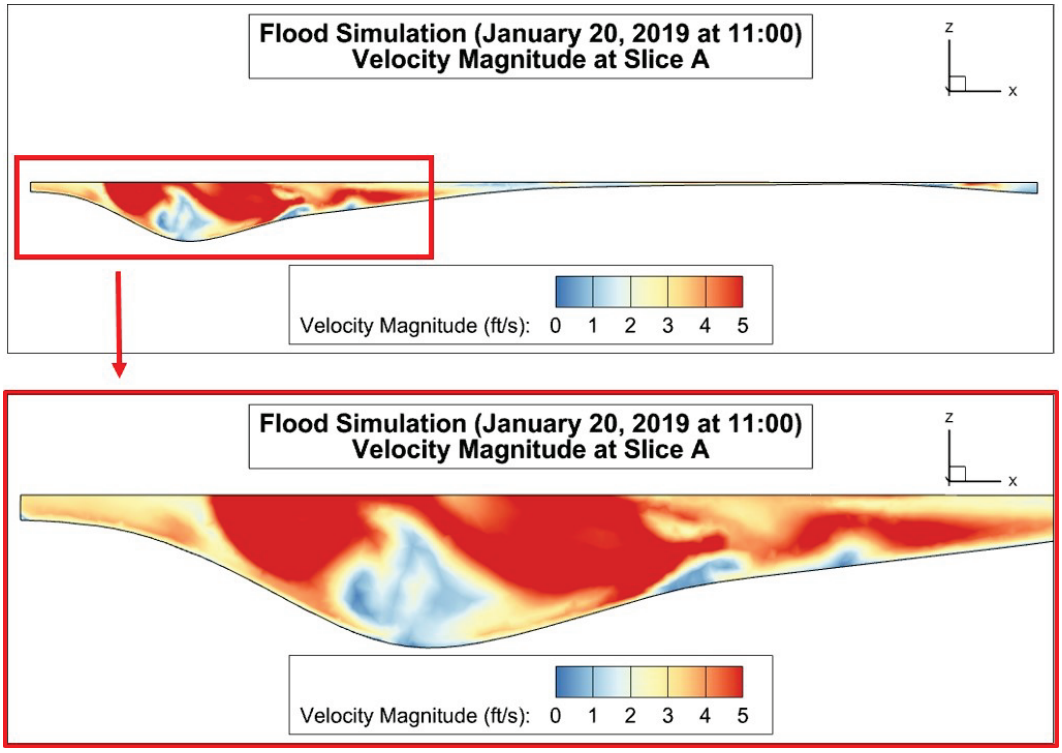

Figure 38. Flood simulation velocity magnitude at vertical Slice B.

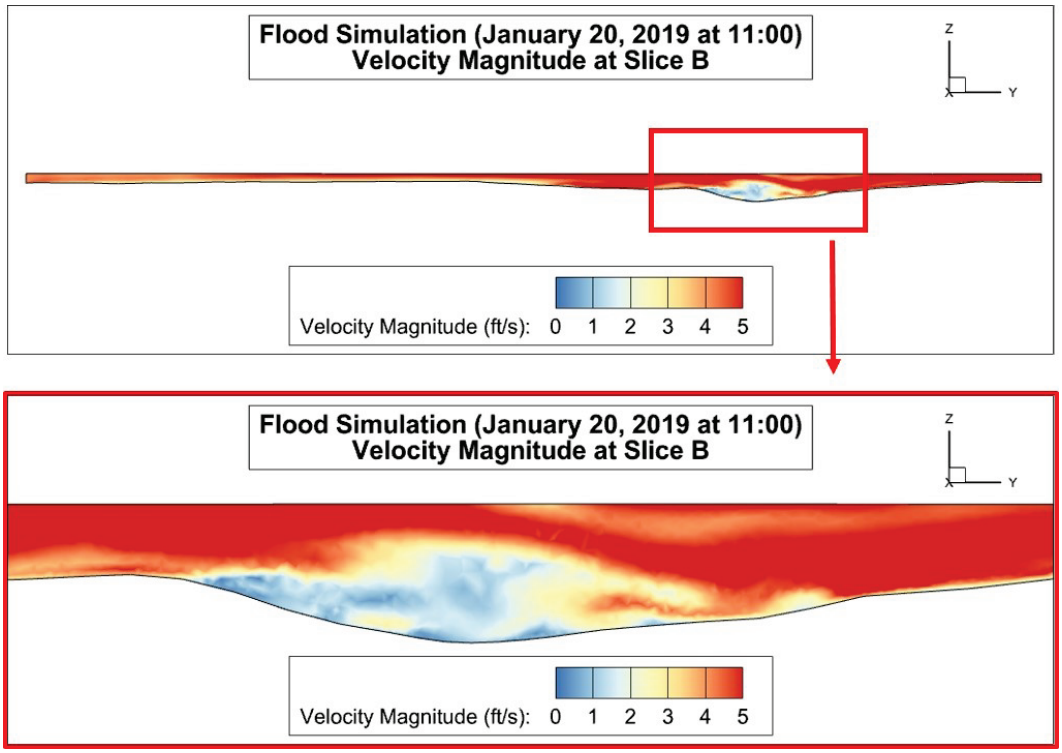

Figure 39. Flood simulation velocity magnitude at vertical Slice C.

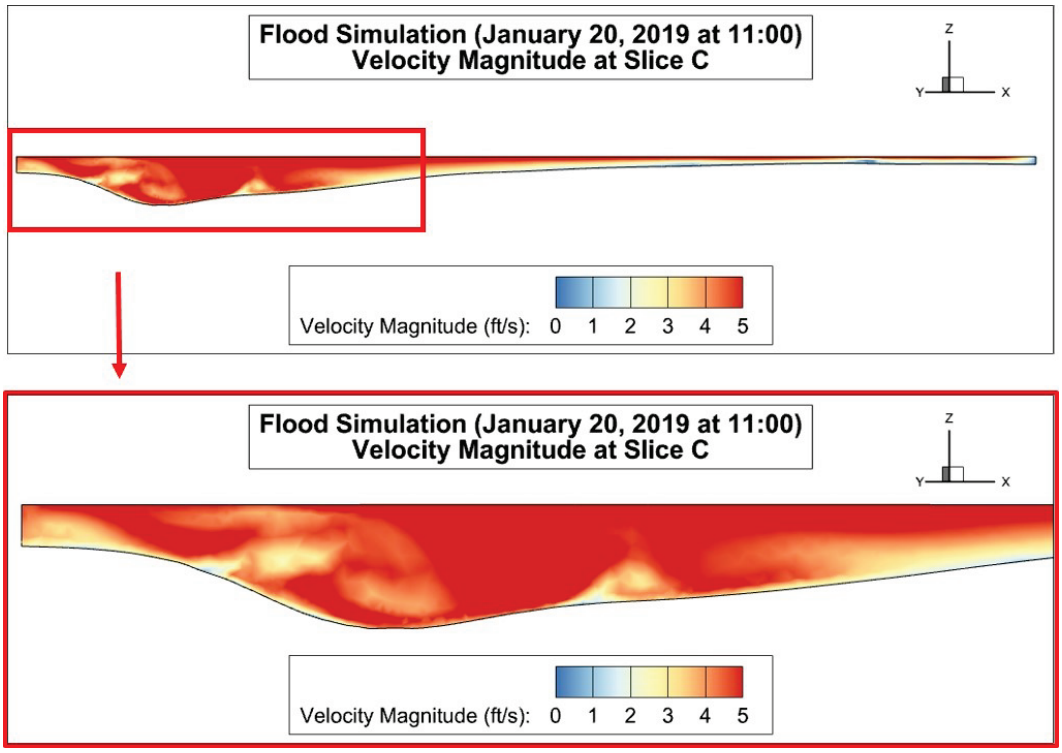

Figure 40. Flood simulation velocity magnitude at vertical Slice D.

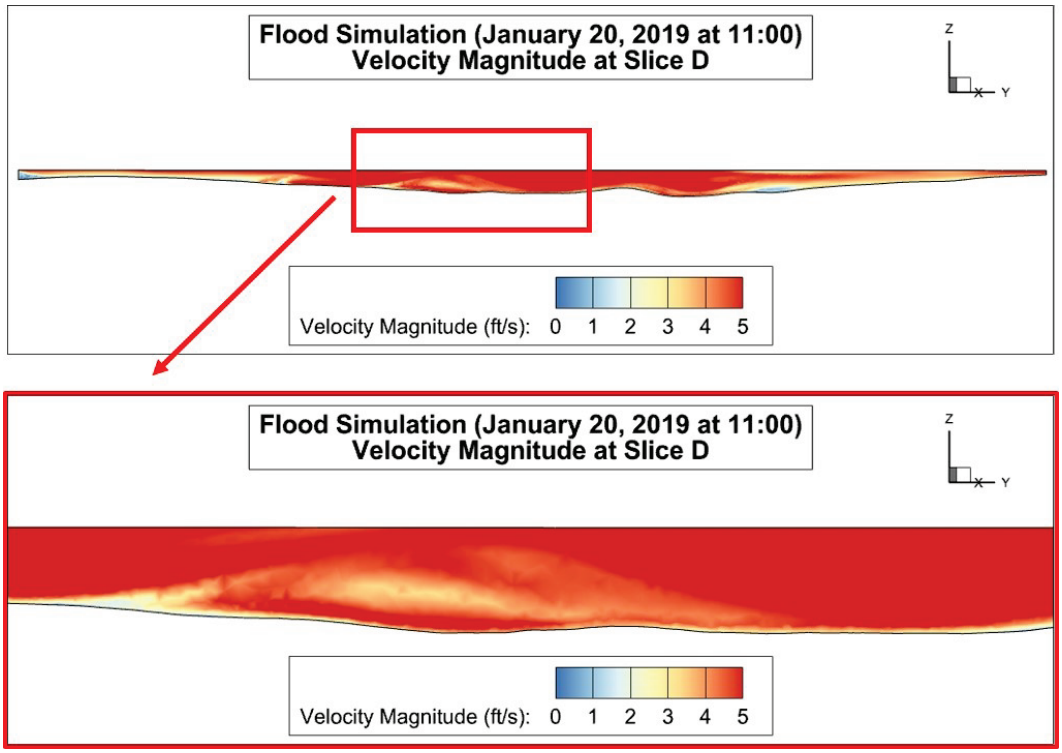

6.2.2 Bed shear stresses

Contour plots of the bed shear stresses for the flood condition are shown in Figure 41 (full domain) and Figure 42 (an enlarged view of the shear stress contours near the areas of interest). The shear stresses were calculated directly from the flow velocities near the bed (see Figure 33 and Figure 34) using Equation 5 during post-processing. As described in Section 6.2.1, the velocities near the inflow (southeastern) boundary are artificially high because of how the velocities at the inflow boundary were specified. Therefore, the shear stresses at the southeast boundary are also artificially high and should be ignored. The contours range from 0.0 to 0.8 lbf/ft^2 with the blue coloring indicating areas with the smallest shear stresses and red coloring indicating areas with the largest shear stresses. The southern area of interest experiences shear stresses up to 0.8 lbf/ft^2, while the northern area of interest experiences shear stresses of us to 0.5 lbf/ft^2. The highest concentration of shear stresses near 0.8 lbf/ft^2 is located along the edge of the flow domain to the north and southwest of the southern area of interest.

Figure 41. Flood condition bed shear stresses.

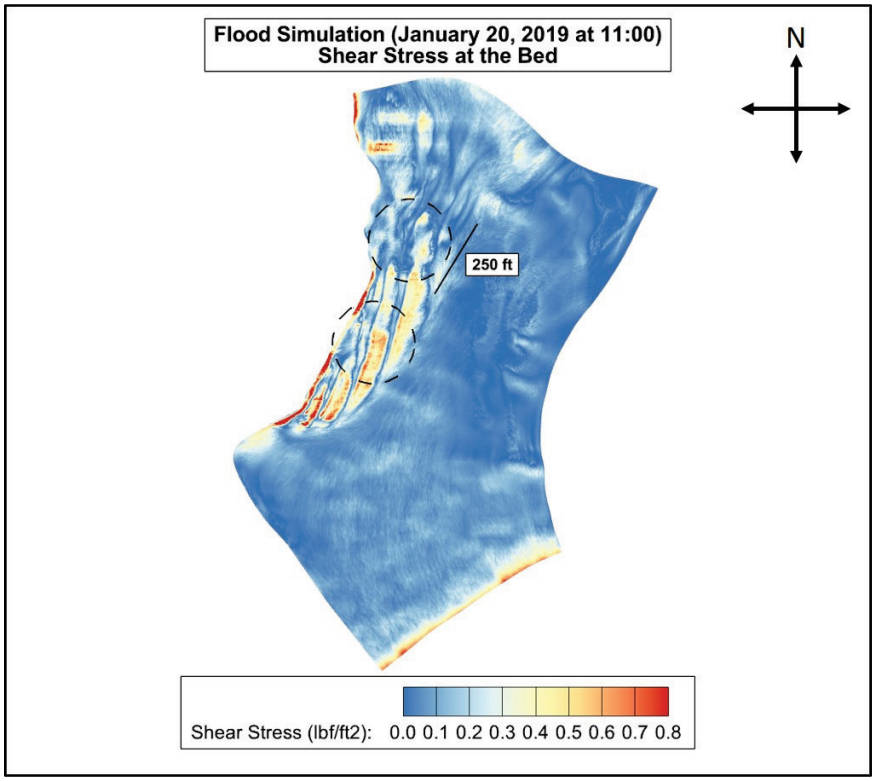

Figure 42. Flood condition bed shear stresses — areas of interest.

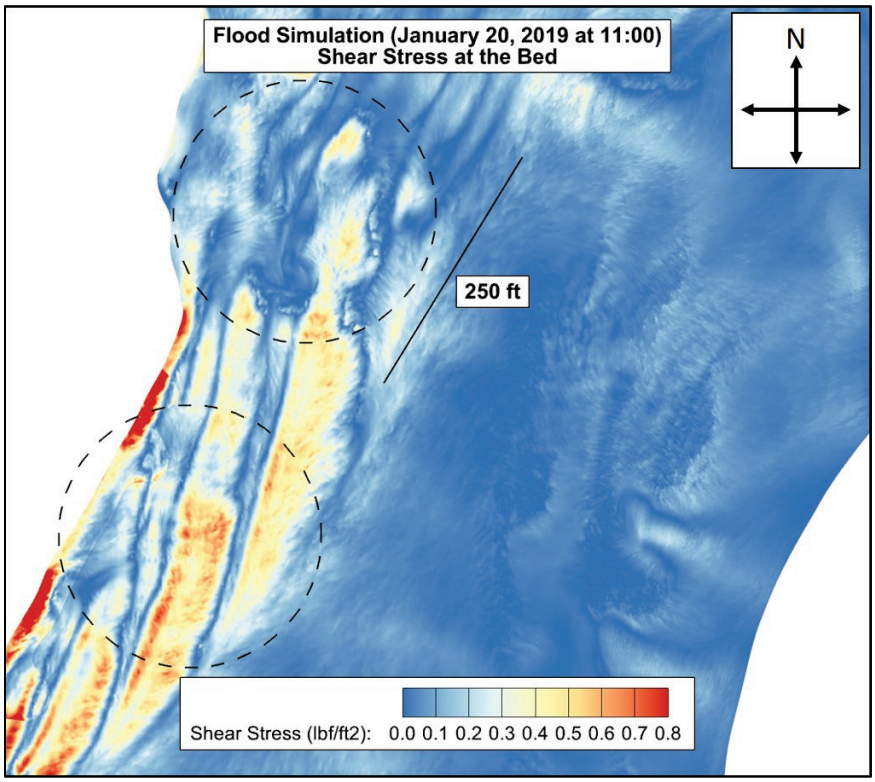

6.3 Ebb flow

6.3.1 Velocity

A contour plot of the velocities near the channel bed for the ebb condition is shown in Figure 43. Figure 44 is an enlarged view of the velocity contour plot for the areas of interest. The velocity range shown in the contours is 0 to 5 ft/s with the blue coloring indicating areas with the smallest velocities and red coloring indicating areas with the largest velocities. The velocities along the inflow (northern) boundary should be ignored because these velocities are a consequence of the velocity applied on this boundary having no vertical variation. The flow is directed generally from the north to the south throughout the flow domain. The flow approaching the northern area of interest converges as the channel narrows because of the area of the channel that is dry at this instance during the tide cycle. The largest bed velocities occur near the northern edge of the northern area of interest. The northern area of interest experiences bed velocities up to 3 ft/s whereas the southern area of interest experiences bed velocities up to 2 ft/s.

Figure 43. Ebb condition bed velocity magnitudes.

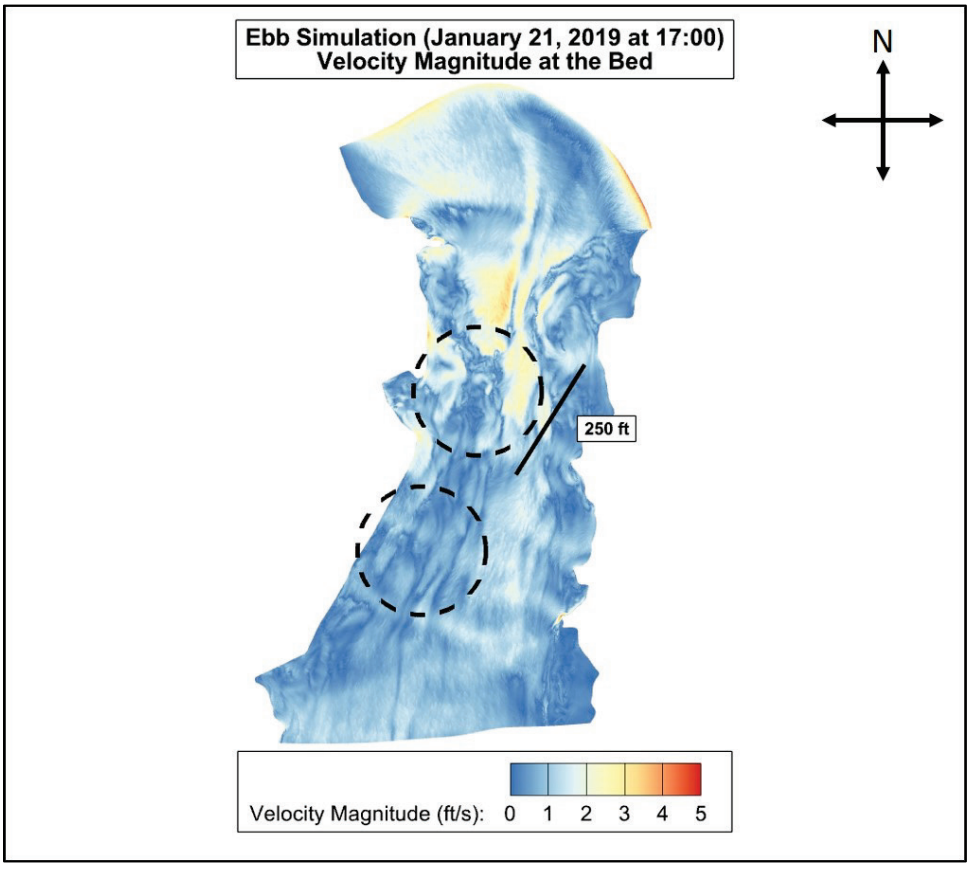

Figure 44. Ebb condition bed velocity magnitudes — areas of interest.

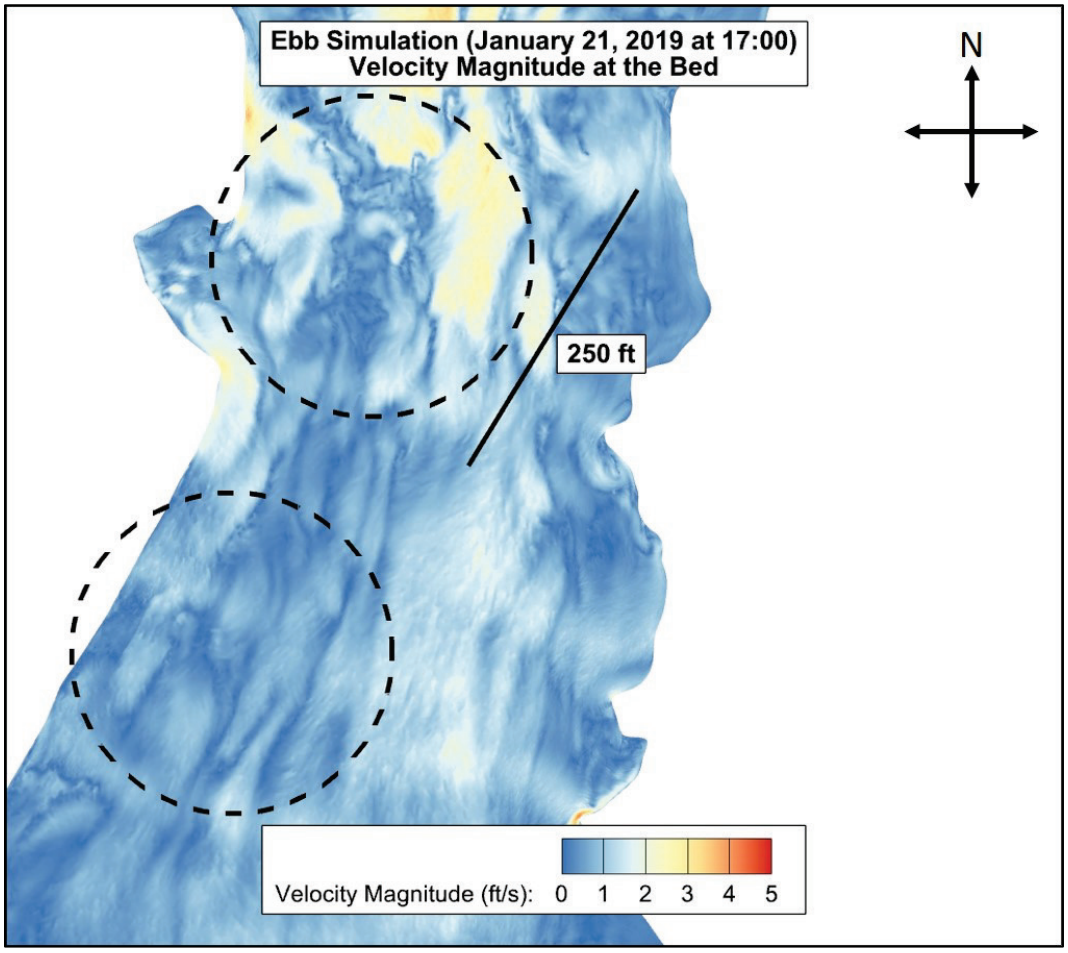

Contour plots of the velocities at the water surface for the ebb condition are shown in Figure 45 (full domain) and Figure 46 (an enlarged view of the velocity contour plot for the areas of interest). The velocity range shown in the contours is 0 to 8 ft/s with the blue coloring indicating areas with the smallest velocities and red coloring indicating areas with the largest velocities. The velocities along the inflow (northern) boundary should be ignored because these high velocities are a consequence of the velocity applied on this boundary having no vertical variation. The highest velocities are in the central (north to south) portion of the flow channel. The water surface flow velocity in the northern area of interest ranges from 0 to 8 ft/s, and the southern area of interest experiences water surface velocities of 1 to 5 ft/s.

Figure 45. Ebb condition water surface velocity magnitudes.

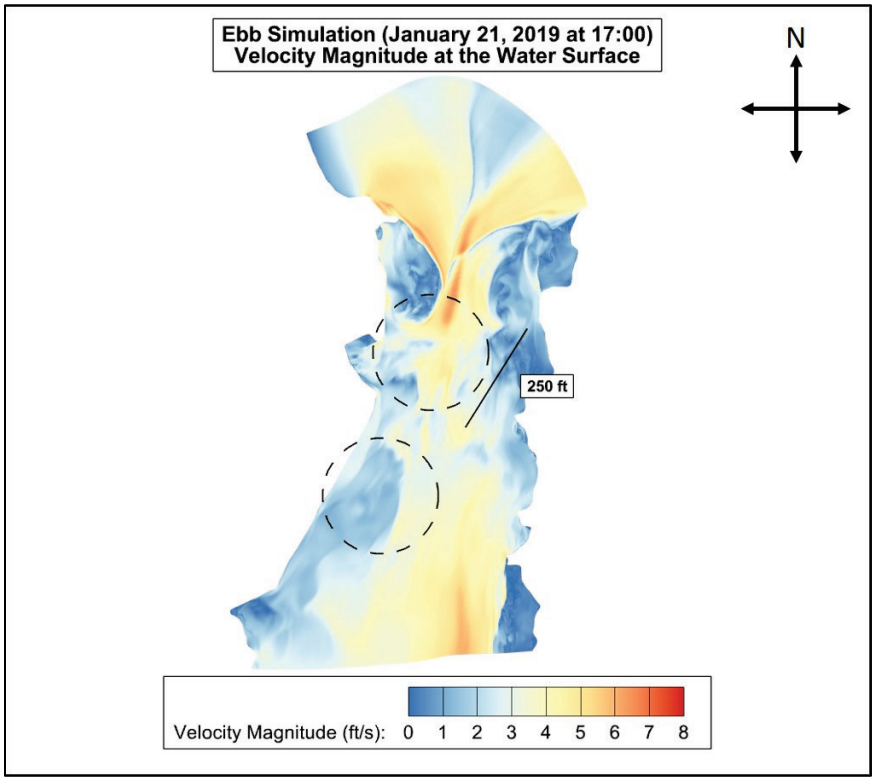

Figure 46. Ebb condition water surface velocity magnitudes — areas of interest.

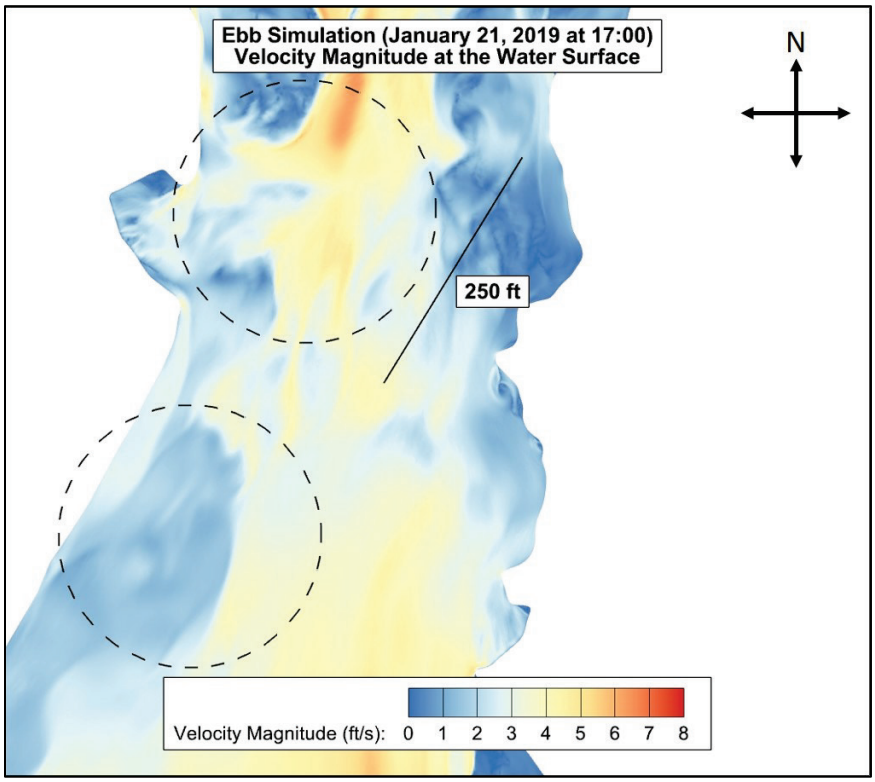

Contour plots showing the velocity distribution along four vertical slices through the areas of interest in the flood domain (see Figure 32) are shown in Figure 47 through Figure 50. The top image in each figure shows the entire slice, and the bottom image is a view of the slice enlarged around one of the areas of interest. The contour range for each plot is 0 to 5 ft/s, with blue coloring indicating velocities near 0 ft/s and the red coloring indicating the velocities near 5 ft/s. The slices through the northern area of interest are shown in Figure 47 (Slice A) and Figure 48 (Slice B). The flow near the area of interest experiences flow velocities of 0 to 3.5 ft/s. The bottom of the scour hole generally experiences velocities of 0 to 1 ft/s with some regions on the inclines of the scour hole experiencing bed velocities as high as 3 ft/s. In regions to the east of the area of interest (to the right in Figure 47), the velocities are much lower (0 to 3 ft/s) throughout the entire water column. The slices through the southern area of interest are shown in Figure 49 (Slice C) and Figure 50 (Slice D). The velocities in the southern area of interest range from 0 to 2 ft/s. Near the channel bed, the velocity ranges from 0 to 1 ft/s.

Figure 47. Ebb simulation velocity magnitude at vertical Slice A.

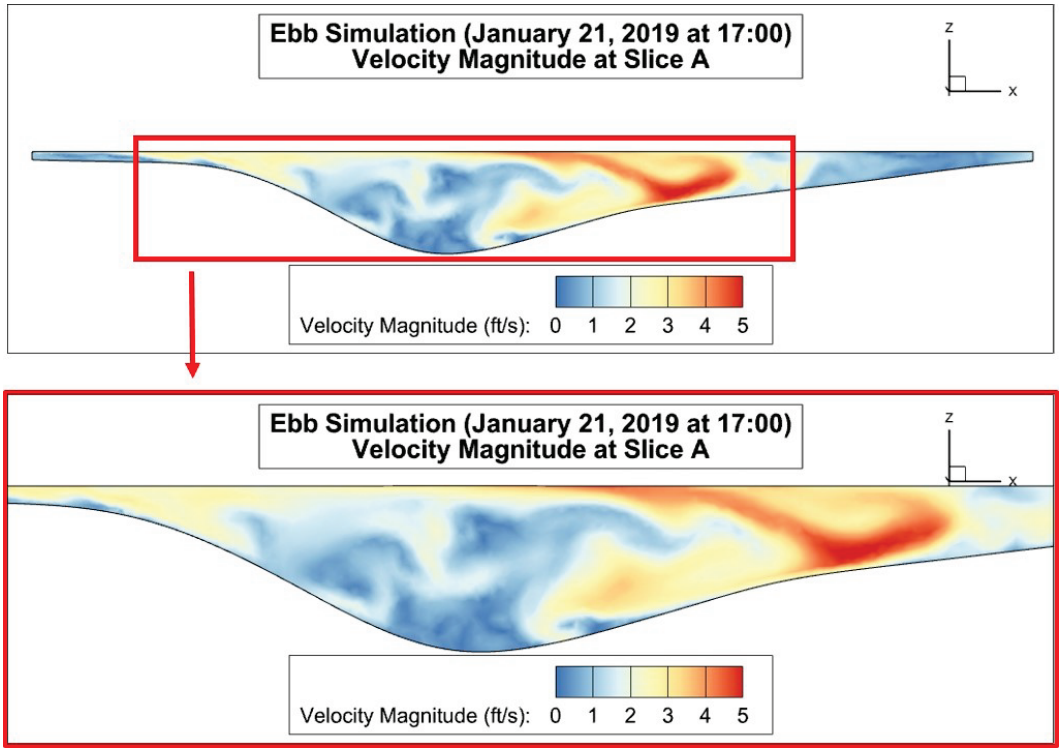

Figure 48. Ebb simulation velocity magnitude at vertical Slice B.

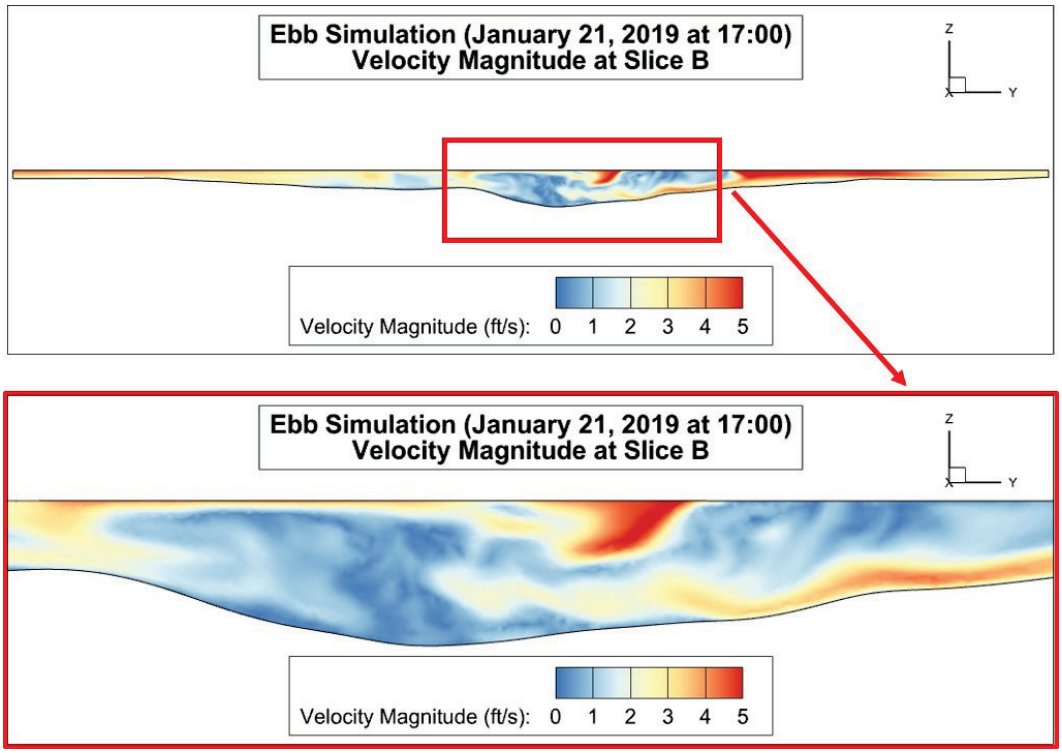

Figure 49. Ebb simulation velocity magnitude at vertical Slice C.

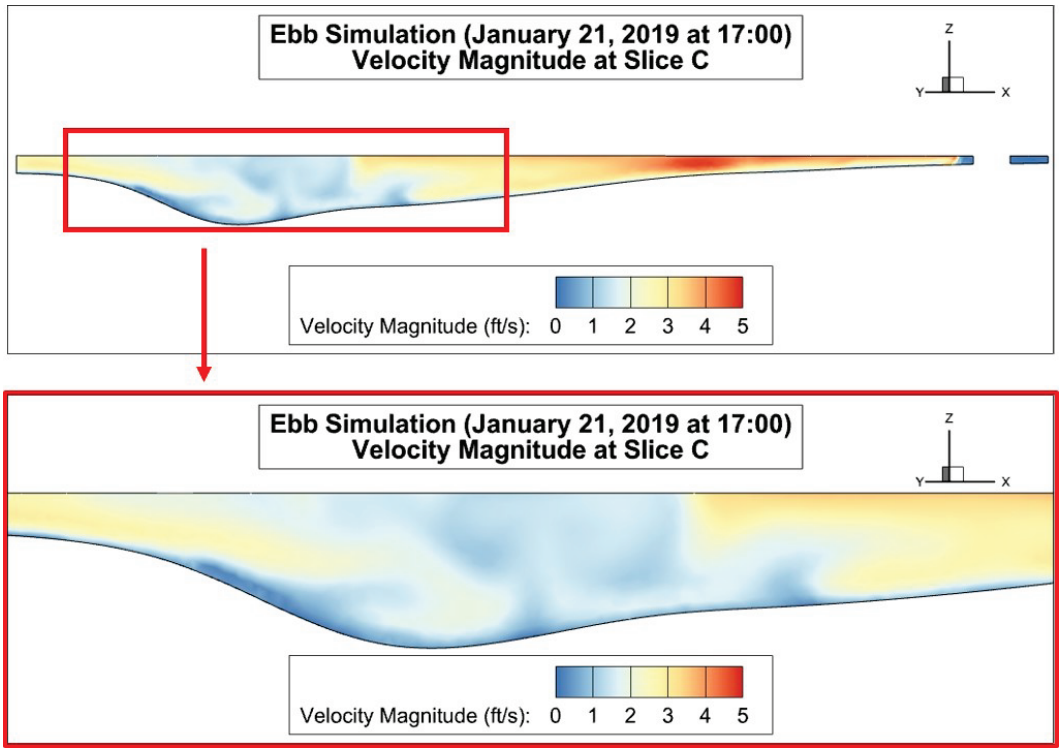

Figure 50. Ebb simulation velocity magnitude at vertical Slice D.

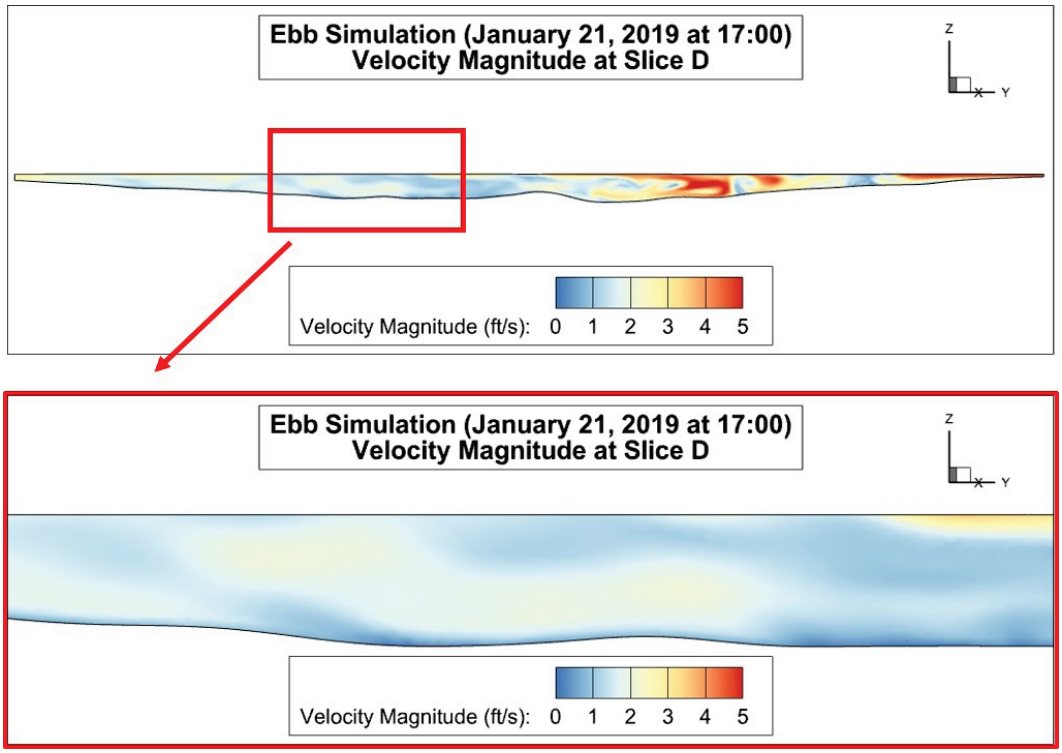

6.3.2 Bed shear stresses

A contour plot of the bed shear stresses for the flood condition is shown in Figure 51. Figure 52 is an enlarged view of the shear stress contours near the areas of interest. The shear stresses were calculated directly from the flow velocities near the bed (see Figure 43 and Figure 44) using Equation 5. As described in Section 6.2.1, the velocities near the inflow (northern) boundary are artificially high because of how the velocities at the inflow boundary were specified. Therefore, the shear stresses at the northern boundary are also artificially high and should be ignored. The contours range from 0.0 to 0.5 lbf/ft^2 with the blue coloring indicating areas with the smallest shear stresses and red coloring indicating areas with the largest shear stresses. The southern area of interest experiences shear stresses up to 0.2 lbf/ft^2, while the northern area of interest experiences shear stresses up to 0.5 lbf/ft^2. The highest concentration of shear stresses near 0.5 lbf/ft^2 is located just north of the northern area of interest.

Figure 51. Ebb condition bed shear stresses.

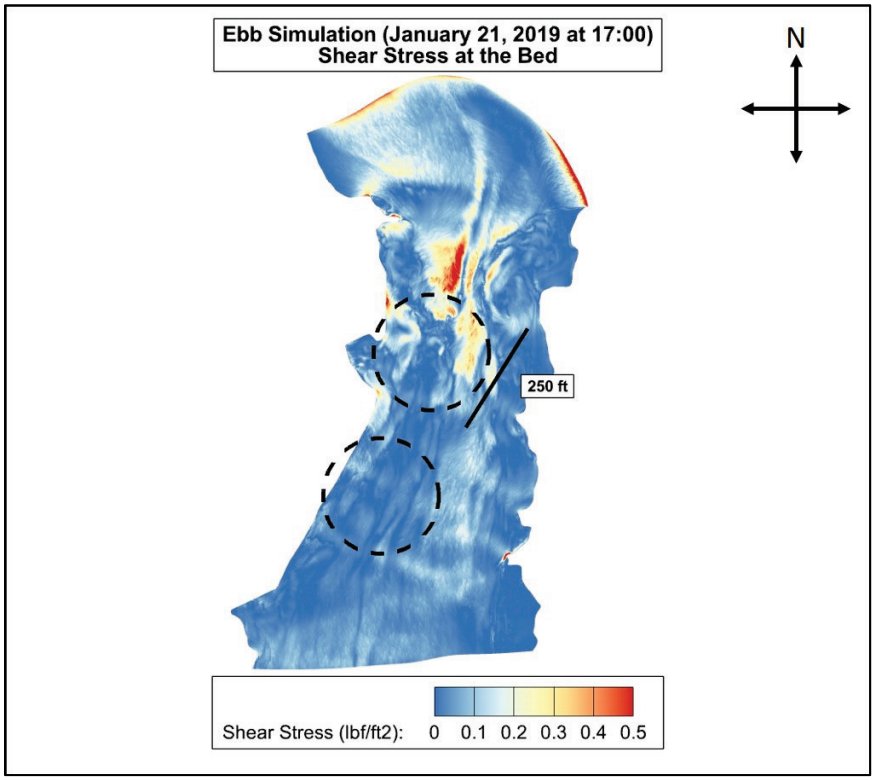

Figure 52. Ebb condition bed shear stresses — areas of interest.

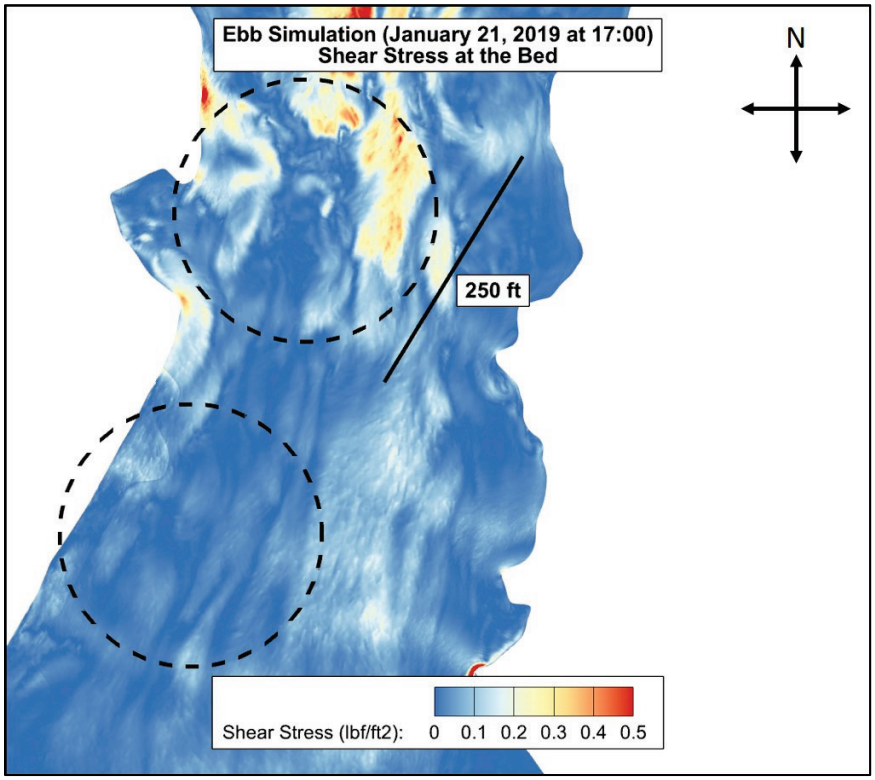

6.4 Comparison of flood and ebb conditions

The flood and ebb conditions produce noticeably different flow behavior throughout the flow domain. These differences are due to the differences in the discharges and flow depths during the two tide conditions and the differences in the predominant direction of flow present during these tides. During the flood condition, the discharge through the flow domain is larger than during the ebb tide, and larger velocities are produced in the areas of interest. The flood condition produces higher bed velocities in the southern area of interest than in the northern area of interest (Figure 33 and Figure 34). Conversely, the ebb condition produces larger bed velocities in the northern area of interest (Figure 43 and Figure 44). The highest bed velocities produced during the flood condition are further west than those produced during the ebb condition.

Figure 37, Figure 38, Figure 47, and Figure 48 show the flow behavior within the scour hole for both flow conditions. Both the flood and ebb conditions produce flows between 0 and 2 ft/s. The flow velocities on the vertical slices through the scour hole show that the highest bed velocities near the bed are on the inclines of the scour hole, indicating that any growth of the scour hole is most likely to occur on the sides of the scour hole instead of its deepest parts. This flow behavior only indicates where scour would most likely occur if scouring begins — not whether scouring will occur. The determination of whether scour will occur requires knowledge of the critical shear stresses for the channel bed material, which was not available to the authors during the study. Figure 39, Figure 40, Figure 49, and Figure 50 show that the flood tide produces much higher flow velocities in the southern area of interest than in the northern area of interest.

The shear stress comparison has the same trends of the velocities near the channel bed. The highest shear stresses are produced by the flood condition in the southern area of interest and along the western boundary of the flow domain (Figure 41 and Figure 42). The ebb condition produces generally lower shear stresses, and the highest shear stresses produced during the ebb tide are just to the north of the northern area of interest (Figure 51 and Figure 52).

7 Summary

A 3D numerical model study has been conducted to determine the flow behavior in a portion of Isle of Wight Bay near Ocean City, MD. This flow behavior will be used to determine if additional bed protection near the western shoreline (including an existing scour hole) should be installed. Two areas of interest (one northern and one southern) along the western shoreline are the focus of the results of this study (Figure 2). Two steady-state flow conditions were determined during this study. These flow conditions correspond to the most extreme flood and ebb tide flow behaviors determined during a previously completed 2D hydraulic model study[1].

The results of this study include flow velocities throughout the flow domain and shear stresses throughout the channel bed for each flow condition. The flood condition produces the flow behavior most likely to produce scour. In the southern area of interest, the flood condition produces velocities near the channel bed up to 5 ft/s and bed shear stresses up to 0.8 lbf/ft^2. In the northern area of interest, the flood condition produces lower velocities near the channel bed and bed shear stresses—4 ft/s and 0.6 lbf/ft^2, respectively. The peak near-bed flow velocities and shear stresses are lower for the ebb condition than for the flood condition. In the southern area of interest, the ebb condition produces velocities near the channel bed up to 2 ft/s and bed shear stresses up to 0.2 lbf/ft^2. In the northern area of interest, the highest velocities near the channel bed and bed shear stresses in the northern area of interest are 3 ft/s and 0.4 lbf/ft^2, respectively.

The flow behavior determined during this study only indicates where scour would most likely occur if scouring begins — not whether or not scouring will occur. These results should be used in conjunction with geotechnical information for the areas of interest in Isle of Wight Bay to determine if additional channel bed protection should be installed.

[1] C. Jared McKnight, Tate O. McAlpin, Keaton E. Jones, and Cassandra G. Ross. In preparation. *Ocean City Inlet, Maryland: A Two Dimensional Shallow Water Adaptive Hydraulics (AdH-SW2D) Hydrodynamic and Sediment Transport Model*, ERDC/CHL Technical Report. Vicksburg, MS: US Army Engineer Research and Development Center.

References

Brunner, Gary, Gaurav Savant, and Ronald Heath. 2020. *Modeler Application Guidance for Steady vs Unsteady, and 1D vs 2D vs 3D Hydraulic Modeling*. TD-41 August 2020. https://www.hec.usace.army.mil/publications/TrainingDocuments/TD-41.pdf

Hammack, Allen, and Morgan Johnston. 2019. *Numerical Model Study of the Flows around Pile Dikes and Conventional Rock Dikes in the Columbia River*. ERDC/CHL TR-19-3. Vicksburg, MS: US Army Engineer Research and Development Center.

Schlichting, H., and K. Gersten. 2000. *Boundary-Layer Theory*. 8th revised ed. New York, NY: Springer.

Wilcox, D. C. 1998. *Turbulence Modeling for CFD*. La Canada, CA: DCW Industries.

Unit Conversion Factors

Multiply	By	To Obtain
cubic feet	0.02831685	cubic meters
feet	0.3048	meters
miles (US statute)	1,609.347	meters
miles per hour	0.44704	meters per second
pounds (force) per square foot	47.88026	Pascals

Acronyms and Abbreviations

2D	Two-dimensional
3D	Three-dimensional
AdH	Adaptive Hydraulics
CAD	Computer-aided design
ERDC	US Army Engineer Research and Development Center
GMT	Greenwich Mean Time
HPC	High-performance computing
NAB	Baltimore District
NAVD88	North American Vertical Datum of 1988
RANS	Reynolds-Averaged, Navier-Stokes
SW2	Two-dimensional Shallow-Water

REPORT DOCUMENTATION PAGE

Form Approved
OMB No. 0704-0188

1. REPORT DATE	2. REPORT TYPE	3. DATES COVERED *(From - To)*
April 2022	Final Report	

4. TITLE AND SUBTITLE
Three-Dimensional Numerical Model Study of Flow near a Scour Hole in Isle of Wight Bay near Ocean City, Maryland

5a. CONTRACT NUMBER

5b. GRANT NUMBER

5c. PROGRAM ELEMENT NUMBER

6. AUTHOR(S)
Allen Hammack and Morgan M. Johnston

5d. PROJECT NUMBER

5e. TASK NUMBER

5f. WORK UNIT NUMBER

7. PERFORMING ORGANIZATION NAME(S) AND ADDRESS(ES)
Coastal and Hydraulics Laboratory
US Army Engineer Research and Development Center
3909 Halls Ferry Road
Vicksburg, MS 39180-6199

8. PERFORMING ORGANIZATION REPORT NUMBER
ERDC/CHL TR-22-7

9. SPONSORING/MONITORING AGENCY NAME(S) AND ADDRESS(ES)
USACE, Baltimore District
Baltimore, MD 21201

10. SPONSOR/MONITOR'S ACRONYM(S)
USACE NAB

11. SPONSOR/MONITOR'S REPORT NUMBER(S)

12. DISTRIBUTION/AVAILABILITY STATEMENT
Approved for public release; distribution is unlimited.

13. SUPPLEMENTARY NOTES
USACE, Baltimore District; MIPR E140

14. ABSTRACT

A scour hole has developed in Isle of Wight Bay near Ocean City, MD. This hole could grow to the point that nearby land developments are threatened, so channel-bed protection measures may be implemented near this scour hole. Appropriately designing those bed protection measures requires knowledge of the flow behavior in the scour hole, so a three-dimensional model study has been conducted to determine the flow behavior at the extreme flood and ebb tides present during a pre-selected month of tide cycles. Steady-state simulations of the flows during those two tide conditions have been completed. Contour plots of the flow velocity near the bed and the corresponding bed shear stresses are provided as input for the design of the bed protection measures.

15. SUBJECT TERMS
Hydraulics—Computer simulation, Hydraulics—Numerical analysis, Isle of Wight Bay (Md.), Scour (Hydraulic engineering), Shore protection, tides

16. SECURITY CLASSIFICATION OF:			17. LIMITATION OF ABSTRACT	18. NUMBER OF PAGES	19a. NAME OF RESPONSIBLE PERSON
a. REPORT	b. ABSTRACT	c. THIS PAGE			Allen Hammack
Unclassified	Unclassified	Unclassified	SAR	72	19b. TELEPHONE NUMBER *(Include area code)* 601-634-3628